FINAL REPORT—DEEP WATER SEDIMENT/PORE WATER CHARACTERIZATION AND INTERACTIONS

MINE WASTE TECHNOLOGY PROGRAM
ACTIVITY IV, PROJECT 9

Prepared by:

Montana Tech of The University of Montana
1300 W. Park Street
Butte, Montana 59701

and

MSE Technology Applications, Inc.
P.O. Box 4078
Butte, Montana 59701

Prepared for:

U.S. Environmental Protection Agency
National Risk Management Research Laboratory
Cincinnati, Ohio 45268
IAG No. DW89938513-01-0

and

U.S. Department of Energy
Federal Energy Technology Center
Pittsburgh, Pennsylvania 15236
Contract No. DE-AC22-96EW96405

December 1999

REVIEWS AND APPROVALS:

Prepared by: _____

Project Engineer

Approved by: _____

Program Manager

December 1999

FINAL REPORT—DEEP WATER SEDIMENT/PORE WATER CHARACTERIZATION AND INTERACTIONS

MINE WASTE TECHNOLOGY PROGRAM ACTIVITY IV, PROJECT 9

Prepared by:

Montana Tech of the University of Montana
Butte, Montana 59701

Dr. L.G. Twidwell (Department of Metallurgical Engineering)
Dr. C. A. Young (Department of Metallurgical Engineering)
Mr. R. J. Ziolkowski (Department of Metallurgical Engineering)
Dr. R.B. Berg (Montana Bureau of Mines and Geology)

IAG NO: DW89938513-01-0

Project Officer

Mr. Roger Wilmoth
Office of Research and Development
National Risk Management Research Laboratory
Cincinnati, Ohio 45268

MSE Technology Applications, Inc.
200 Technology Way
P.O. Box 4978
Butte, Montana 59702

Foreword

Today, industries are developing and modifying technologies to more efficiently produce their products. The waste generated by these industries, if improperly dealt with, can threaten public health and degrade the environment. The U.S. Environmental Protection Agency the (EPA) is charged by Congress with protecting the nation's land, air, and water resources and under mandate of national environmental laws, the EPA strives to formulate and implement actions leading to a balance between human activities and the ability of natural systems to support and nurture life. These laws direct the EPA to perform research to define and measure the impacts and search for solutions to environmental problems.

The National Risk Management Research Laboratory (NRMRL) of the EPA is responsible for planning, implementing, and managing research, development, and demonstration programs to provide an authoritative, defensible engineering basis in support of the policies, programs, and regulations of the EPA with respect to drinking water, wastewater, pesticides, toxic substances, solid and hazardous wastes, and Superfund-related activities. The Federal Energy Technology Center (FETC) of the U.S. Department of Energy (DOE) has responsibilities similar to the NRMRL in that FETC is one of the several DOE centers responsible for planning, implementing, and managing research and development programs. In June 1991, an Interagency Agreement was signed between the EPA and DOE that made funds available to support the Western Environmental Technology Office's operating contractor, MSE Technology Applications, Inc., and Montana Tech of The University of Montana (Montana Tech) for the development of the Mine Waste Technology Program (MWTP). This publication is one of the products of the research conducted by the MWTP through these two federal organizations and provides a vital communications link between the researcher and the user community.

The objectives of Activity IV, Project 9 were to collect Berkeley Pit deep water sediments, to characterize the resident conditions in deep water sediments, and to model the collected data to understand the formation of deep water sediments. The results of this study will help in the future design of treatment processes for cleanup of large acid mine water storage lakes.

This experimental test program was conducted at Montana Tech and was directed by Drs. L.G. Twidwell (Department of Metallurgical Engineering), C.A. Young (Department of Metallurgical Engineering), and R.B. Berg (Montana Bureau of Mines and Geology). The graduate student who assisted the test program was Mr. R.J. Ziolkowski (Department of Metallurgical Engineering). This final report was written by the above participants.

Executive Summary

Montana Tech of the University of Montana (Montana Tech) and MSE Technology Applications, Inc. (MSE) are involved in a coordinated series of studies to delineate the characteristics of the Berkeley Pit lake located in Butte, Montana. The project objectives are to summarize available information, to generate new information needed to formulate a conceptual environmental model for the Berkeley Pit lake, and to provide characterization data for the development of advanced treatment technologies. The project described in this report is one of the subsystems of the environmental model, i.e, the characterization of deep water and deep water sediments/pore water. Other component programs include the evaluation of the characteristics of the Pit lake surface water (C. A. Young, Metallurgical Engineering Department); the characterization of the Pit lake water column elemental concentrations (J. Jonas, Chemistry Department); the evaluation of the organic components present in the Pit lake water (D. Cameron, Chemistry Department); and the evaluation of the presence of biological constituents in the Pit lake water (G. Mitman, Biology Department).

Study Objectives

The objectives of the deep water sediment/pore water characterization and interaction study are presented below. Each objective has been successfully completed.

Collection of deep water upper layer sediment samples—Deep water samples and surface sediment samples were collected during a sampling campaign in November 1997. Samples were collected from the 600- and 700-foot (ft) water depths.

Collection of subsurface sediment/pore water samples—Three sediment core samples were collected during a sampling campaign in April 1998 from a water depth of 717 ft.

Characterization and speciation of sediment solids and subsurface pore water—The sediment solids and pore waters were chemically characterized as a function of sediment depth.

Modeling the system to understand the controlling sediment formation reactions—Modeling of the deep water and sediment/pore waters was initiated. Compounds were identified that likely are controlling the elemental concentrations for aluminum, arsenic, calcium, ferric iron, potassium, and silicon.

Study Conclusions

Deep Water

There does not appear to be significant differences in the elemental content of the upper water column and the deep water (near-sediment) solution. However, iron shows a slight (approximately 5%) increase in concentration with depth (from surface to 717 ft). The ferrous-to-ferric ratio shows a marked increase from the surface to approximately 100 ft; the ratio remains constant from 100 to 717 ft.

Phosphate, nitrate, and nitrite concentrations were found to be less than the detection limit at all depths. Fluoride [approximately 30 to 40 parts per million (ppm)] and chloride (approximately 10 to 15 ppm)

concentrations were relatively constant with depth. Sulfate showed a generally increasing concentration as a function of water depth, e.g., 8.7 grams per liter (g/L) at 2 ft and 9.5 g/L at 715 ft.

The in situ measured dissolved oxygen concentration was relatively high near the surface; it then dropped dramatically from 2 to 18 ft then rose to levels exceeding the level near the surface. The concentration then became relatively constant with increasing depth from approximately 100 ft to near the sediment surface. The data appears to suggest that surface water turnover may have occurred down to the 100-ft level. The collection of additional data is required to confirm this preliminary conclusion.

Sediment Solids and Pore Water

The following conclusions concerning the sediment pore water and solids have been drawn from the characterization studies.

Pore Water

Pore water is the water present within the sediment. This water was separated as a function of depth into a series of sediment core samples. The pore water was not clean (at least to the sediment depths studied in this investigation) and had an appreciable elemental content.

Pore waters had a lower concentration of aluminum, arsenic, potassium, and phosphorus than the deep water 1 meter above the sediment surface. The aluminum, arsenic, potassium, and phosphorus concentration in the pore waters remained approximately constant throughout each sediment core length.

Pore waters had a higher concentration of copper, iron, and sulfur than the deep water. The pore water concentration depth trends for each element are as follows.

- Copper concentrations at the top of the cores were essentially the same as in the deep water, but the copper concentration approximately doubled in the lower sediment pore waters.

- Iron concentrations at the top of the cores were approximately double the iron concentration in the deep water, but the iron concentrations in the pore waters decreased with core depth to approximately the same concentration as in the deep water.

- Sulfur concentration at the top of the cores was higher than in the deep water, but the concentration of sulfur in the pore waters decreased with core depth to approximately the same concentration as in the deep water.

Pore waters had essentially the same concentration (within 10%) as the deep water for calcium, magnesium, manganese, sodium, silicon, and zinc.

Ferrous concentrations in the pore water were approximately four times higher in concentration in the upper sediment layers than in the deep water. The ferrous concentrations decreased with core depth from approximately 2.4 to 2.7 g/L in the upper layers of the cores to approximately 1.0 to 1.2 g/L in the deepest layers. The reaction of potassium jarosite ($KFe_3(SO_4)_2(OH)_6$) and/or schwertzmannite ($Fe_8O_8(OH)_6SO4$,) with organic carbon to form ferrous species appears to be feasible for the conditions

existing in the sediments and is the likely reaction controlling the ferrous concentration in the pore water.

Ferric concentrations in the pore water were approximately one-half as high in concentration in the upper sediment layers than in the deep water. The ferric concentrations varied with core depth but contained an average ferric concentration of 174±72 milligrams per liter (mg/L).

Sediment Solids

Sediment solids showed varying composition trends. Elements that showed definite decreasing concentration trends with core depth included arsenic, calcium, iron, magnesium, phosphorus, lead, and sulfur.

The sediment solids were composed of detrital and precipitated compounds. The major detrital compounds were quartz, biotite, and muscovite. The major precipitated compounds were jarosite and gypsum. Jarosite and gypsum concentrations were highest in the upper portion of the sediment layer and decreased with depth into the sediment layer.

There was a trend in the mix of precipitated and detrital material with depth, i.e., the precipitated compounds were present at a higher concentration at the surface of the core. This noted trend suggests that precipitated solids formed in the water column and settled to the sediment surface. With time, wall rock joined the sediment and diluted the sediment with detrital compounds.

Modeling

The concentration of individual elements in the pore water can be explained by modeling the solubility of various compounds known to be present in the sediment solids. The modeling effort for this project was initiated. Further modeling results will be forthcoming as a part of the Master of Science thesis presently being prepared by Mr. R. J. Ziolkowski. The modeling results presented in this report are considered to be preliminary results, and more detailed considerations of the experimental data may alter some of the final conclusions.

The results of equilibrium modeling of the sediment/pore water system suggests that the following compounds are likely responsible for controlling the solution elemental concentrations.

- The compound likely responsible for controlling the dissolved aluminum concentration in the sediment/pore water is muscovite ($KAl_3Si_3O_{10}(OH)_{2(M)}$). The compound responsible for controlling the dissolved aluminum concentration in the water column has not yet been defined.

- The compound likely responsible for controlling the dissolved arsenic concentration in the sediment/pore water is ferrous arsenate ($Fe_3(AsO_4)_2$). The compound responsible for controlling the dissolved arsenic concentration in the water column has not yet been defined.

- The compound likely responsible for controlling the dissolved calcium concentration in the sediment/pore water and the water column is gypsum ($CaSO_4.2H_2O$).

- The compound likely responsible for controlling the dissolved ferric concentration in the sediment/pore water and the water column is schwertzmannite ($Fe_8O_8(OH)_6SO_4$). Further investigations are required to support this preliminary conclusion.

- The compound likely responsible for controlling the dissolved potassium concentration in the sediment/pore water is muscovite ($KAl_3Si_3O_{10}(OH)_{2(M)}$). The compound likely responsible for controlling the dissolved potassium concentration in the water column is potassium jarosite ($KFe_3(SO_4)_2(OH)_6$).

- The compound likely responsible for controlling the dissolved silicon concentration in the sediment/pore water is muscovite ($Kal_3Si_3O_{10}(OH)_{2(M)}$). The compound likely responsible for controlling the dissolved silicon concentration in the water column is silica (SiO_2).

As stated above, additional modeling work will be performed. The results of the additional work will be published as a Master of Science thesis in the Metallurgical Engineering Department at Montana Tech as an addendum to the present report.

Contents

Contents (Cont'd)

Figures

Tables

Abbreviations, Acronyms, and Symbols

AA	atomic absorption
AAS	atomic absorption spectroscopy
BPD	Berkeley pit deep
CCB	continuing calibration blanks
CCV	continuing calibration verification
CRDL	contract required detection limit
DO	dissolved oxygen
DOE	U.S. Department of Energy
DL	detection limit
EDX	energy dispersive x-ray
E_H	oxidation-reduction potential relative to H_2
EPA	U.S. Environmental Protection Agency
I	ionic strength
IAG	interagency agreement
ICB	initial calibration blanks
ICP	inductively coupled plasma emission spectrometer
ICSA	interference check samples A
ICSAB	interference check samples A and B
ICV	initial calibration verification
IDL	instrument detection limit
LAP	laboratory analytical protocols
LCS	laboratory control sample
MBMG	Montana Bureau of Mines and Geology
MDL	method detection limits
MWTP	Mine Waste Technology Program
ppb	parts per billion
ppm	parts per million
QA/QC	quality assurance/quality control
QAPP	quality assurance project plan
RPD	relative percent differences
RSD	relative standard deviation
SOP	standard operating procedures
SRM	standard reference material
TCLP	toxicity characteristic leaching procedure
XRD	x-ray diffraction
? G^o	standard free energy

1. Introduction

This final report presents the information and results compiled by Montana Tech of The University of Montana (Montana Tech) for the Mine Waste Technology Program (MWTP), Activity IV, Project 9, Deep Water Sediment/Pore Water Characterization and Interactions. The research described in this report was conducted in accordance with the requirements of the Interagency Agreement (IAG), Activity IV, Scope of Work. The IAG was signed in June 1991 by the U.S. Environmental Protection Agency (EPA) and the U.S. Department of Energy (DOE) to initiate work on the MWTP. The work plan for the MWTP, Activity IV, Project 9 addresses testing and evaluation of technologies applicable to remediation of the EPA technical issue, Mobile Toxic Constituents—Water. The analytical methods and bench-scale treatment testing conducted for this study were consistent with the requirements of the EPA as outlined in the project-specific quality assurance project plan (QAPP) for the deep water sediment/pore water characterization and interactions (Ref. 1). This final report describes the work conducted and summarizes the technical results obtained to evaluate Berkeley Pit lake deep water sediments and resident conditions. Refer to the QAPP for the detailed descriptions of the process operations.

Berkeley Pit lake water has been sampled and analyzed periodically since 1984. The Pit water is acidic and contains elevated concentrations of metal ions. Past sampling events collected water for testing various treatment technologies—the intent of the past sampling has never been to systematically characterize the water at different collection points and at different depths. An exception to this was one preliminary evaluation of water chemistry with depth performed by Davis and Ashenber in the late eighties; however, this study did not include sampling of solids and sediments (Ref. 2). Except for the Davis study, all sampling events have been coordinated and performed by the Montana Bureau of Mines and Geology (MBMG) which is located on the Montana Tech campus in Butte, Montana. This data was summarized (for various independent sampling events) by Metesh and Duaime.[1]

Precipitates and sediments have generally not been collected for characterization. One exception to this is the work of Robins in 1995 (Ref. 3). Robins collected a scoop sample of sediment from the 700-foot (ft) level (distance below the surface of the water) near the center of the Pit by using a drag device. Solids were recovered, but pore water was not recovered. Solids were not completely characterized, but quartz, gypsum, and magnetite were identified.

Robins, et al. (Ref. 3) summarized what was presently known about Berkeley Pit sediment formation prior to this study:

> "Until 1995 there had been no determination of the rate of formation, composition, depth or even the existence of the sediment in the Berkeley Pit. There has been conjecture that the depth of sediment could be as great as 200 ft, and that beneath the sediment surface there was likely to be an oxidation-reduction boundary with respect to a sulfate-sulfide interface. This oxidation-reduction boundary could develop due to the interaction of pore water with underlying sulfide minerals and solutions and also by the possible mediation by sulfate reducing organisms, the former being similar to the supergene enrichment process by which the original supergene

[1] J. Metesh and T. Duaime (MBMG), Memorandum to J. Steinmetz (Director, MBMG), Berkeley Pit profile Data, October 1, 1996.

ore body was formed. In July 1993 a copper bar was dropped onto the sediment at a depth of about 500 ft, and recovered one month later to show a black surface film which produced a positive sulfur analysis.

> In May 1995 a scoop sample of the sediment was taken at a depth of 700 ft in what was originally the deepest part of the open pit. The sample which possibly came from the top 9 inches of the sediment had a wide variation in particle size from about 1-200 µm. This sample has been examined by optical microscopy, x-ray diffraction, x-ray fluorescence, and wet chemical methods. The material consisted mostly of complex silicates. It is interesting to compare a "majors" analysis (on an oxide basis) for the sediment (SED), to that for Butte quartz monzonite (BQM) as follows, with all iron expressed as iron(III):

%	SiO_2	Al_2O_3	Fe_2O_3	MgO	CaO	K_2O	Na_2O			MnO	TiO_2
										P_2O_5	SO_4
SED	59.1	15.31	6.37	1.70	1.77	4.73	1.31	0.09	0.68	0.27	7.2
BQM	64.92	15.46	7.81	2.05	4.24	3.94	3.06	0.09	0.53	0.18	0.15

> A comparison of the K:Na and Ca:Mg ratios, in particular, for the sediment and Butte quartz monzonite, indicate that chemical precipitation has been important in sediment formation. The synthesis of several silicates which are similar to those in the sediment has been accomplished by chemical precipitation in the laboratory, as reported by Harder (Refs. 4, 5).
>
> Constituents of the sediment from the Berkeley Pit were quartz, magnetite, some sulfides and some sulfates.
>
> A culture from the sediment was positive for sulfate reducing bacteria."

Mr. R. B. Berg has performed a preliminary examination of the Robins sediment.[2] Mr. Berg has evaluated the sample with respect to whether the material is consistent with Pit wall mineralogy. His results suggest that most of the sediment is from the Pit wall, "Preliminary examination of one sediment sample shows it to consist mainly of minerals derived from the Pit walls. These are quartz (both from vein quartz, as recognized by abundant fluid inclusions and from the altered granite), K-feldspar, plagioclase, biotite, trace zircon. In addition to minerals derived from the wallrock, small (45 micron) gypsum prisms are a component of this sample."

X-ray diffraction (XRD) analysis of the Robins sediment showed the presence of quartz (SiO_2, PDF# 33-1161) and several silicate minerals, e.g., muscovite-3 [$(K,Na)(Al,Mg,Fe)_2(Si_{3.1}Al_{0.9}O_{10})(OH)_2$, PDF # 07-0042] , and muscovite-1 [$(K)(Mg)(Si_4AlO_{10})(OH)_2$, PDF# 21-0993]. Other mineral phases are also likely to be present in the sediment; however, a more complete evaluation and identification has yet to be performed. The above minerals were present in the coarser fraction of the sediment, which indicates they are likely from the sidewall material rather than from precipitation reactions. However, precipitation reactions are not ruled out because the work of Harder (described below) shows that precipitated clays may be formed under reducing conditions.

Harder (Refs. 4, 5) has demonstrated that silica and iron silicate minerals with clay structures can be formed at low temperatures (3 EC to 20 EC) in a reasonably short time (a few days) if the environmental conditions are reducing and ions such as ferrous, zinc or magnesium are present

[2] R.A. Berg (MBMG), Memorandum to L Twidwell and C. Young (Metallurgical Engineering Department, Montana Tech), September 20, 1996.

along with low concentrations of silicic acid [- <100 parts per million (ppm)]. Reducing conditions, ferrous species, and silicon species were anticipated to be present in deep Berkeley Pit lake water. Whether such clays can be formed from Berkeley Pit lake water has not yet been demonstrated.

Two sampling campaigns were performed during the present study. The first sampling campaign was performed November 18 and 20, 1997. The attempts to collect core samples were unsuccessful. However, deep water and surface sediment solids were successfully recovered. A second sampling campaign was conducted April 22 and 23, 1998. This sampling campaign included the collection of water column samples (results reported elsewhere) and three sediment core samples from the deepest location in the Berkeley Pit. The results from both sampling campaigns are presented and discussed in this report.

2. Objectives of Present Study

The objectives of the present study included the following.

- Collecting deep water upper layer sediment samples.
- Collecting subsurface sediment/pore water samples.
- Characterizing and speciating sediment solids and subsurface pore water.
- Modeling the system to understand the controlling sediment formation reactions.

3. Technical Program

3.1 Background

Montana Tech has embarked on a coordinated series of studies to delineate the characteristics of the Berkeley Pit lake located in Butte, Montana. The objectives of the overall project are to summarize presently available information and to generate new information needed to formulate a conceptual environmental model for the Pit lake. The project described in this report is one of the subsystems of the environmental model.

- Other component programs include an evaluation of the characteristics of the Pit lake surface water (C. A. Young, Metallurgical Engineering Department);
- a characterization of the Pit lake water column elemental concentrations (J. Jonas, Chemistry Department);
- an evaluation of the organic components present in the Pit lake water (D. Cameron, Chemistry Department); and
- an evaluation of the presence of biological constituents in the Pit lake water (G. Mitman, Biology Department).

Samples collected for the deep water sediment/pore water characterization study were shared with the above investigators. Experimental results were shared and periodically discussed. Interactions between principal investigators and graduate students are reflected in the final reports from each component.

The report presented here is not considered the final endproduct of this investigation. Further test work and evaluative research are planned as a part of the Master of Science thesis program being conducted by R. J. Ziolkowski (Ref. 6).

3.2 Research Approach

The approach taken in this study consisted of the following investigations.

Collection of Samples—Collection of deep water from the upper surface of the sediment and collection of core samples containing sediment solids and pore waters were performed. Sample collection was coordinated and performed by the MBMG. Samples were collected in a manner to preserve deep water resident conditions.

Sample Handling and Sample Identification—Water and core samples were transferred to an argon atmosphere prior to subsequent sample subdividing. Water samples were sealed under argon, and core samples were segmented into subsamples, loaded into argon filled containers, and stored at 4 C.

Characterization of Waters and Sediments—Deep water and pore water were analyzed for elemental content (by inductively coupled plasma (ICP) spectrometry), and iron was speciated. Core solids were characterized for elemental composition (by dissolution and ICP spectrometry), for mineralogical content (by XRD), for phase and particulate elemental content [by scanning electron microscopy-energy dispersive x-ray (SEM-EDX)], and for mineralogical content (by optical microscopy).

Modeling of Pore Water Resident Conditions— Sediment solids and pore water were modeled to determine the phases controlling the solubility of major constituents.

3.3 Experimental Procedure

Details of the work plan and quality assurance project plan (QAPP) are presented elsewhere (Refs. 7 and 1, respectively). The experimental procedures used in this study are briefly presented in sections, 3.3.1, Sample Collection; 3.3.2, Sample Handling; and 3.3.3, Characterization of Waters and Sediments.

3.3.1 Sample Collection

All samples were collected by the MBMG under the supervision of Mr. T. Duaime. Deep water and sediment sample collections were performed in two campaigns, i.e., a preliminary effort (November 1997) was conducted to evaluate sampling procedures, and a second effort (April 1998) was conducted using the expertise of the National Water Research Institute, Centre for Inland Waters (Dr. Alena Mudrock and Mr. M. Mawhinney) for retrieving core samples from deep water environments.

Preliminary Sampling Effort—The MBMG attempted to collect deep water and sediment samples November 18 and 20, 1997. A core sampling device and a vertical water sampler were used in the sampling attempt. Two depths were investigated, i.e., one site was at a water depth of 600 ft, and the second site was at a water depth of 700 ft. The retrieval of two deep water samples was successful. The retrieval of core samples was unsuccessful. Only a relatively small amount of solids were recovered in the core sampling device. The solids recovered are considered to be deep water/sediment surface solids.

Second Sampling Effort—A second major (and more successful) sampling effort was conducted by the MBMG April 22 and 23, 1998. Assistance was supplied by Dr. A. Mudrock and Mr. M. Mawhinney from the National Water Research Institute, Centre for Inland Waters. Dr. Mudrock supplied two types of sampling devices: the NISKEN vertical samplers for collecting deep water samples and the Benthos core sampling devices (both devices are described in Appendix A), and a protected environment core extraction device (shown in accompanying photographs in Appendix A).

Three core samples and one deep water sample were retrieved from essentially the same site. The location of the sampling site was Latitude 46E 01' 03.50", Longitude 112E 30' 41.00" at a sediment/water surface depth of 717 ft. One core was recovered April 22 (designated Core One); two cores were recovered April 23, 1998 (designated Core Two and Core Three).

Core One—Core One was collected in the Benthos sampler (a deep water sample was collected in a NISKEN vertical sampler attached 1 meter above the core sampler). The recovered core length was 70 centimeters (cm) with the top 10 cm being mostly water. The core sampling device was capped on both ends, and each end was enclosed in an anaerobic bag. The core was then transported to the Montana Tech Metallurgical Engineering laboratory for sample retrieval.

Core Two—Core Two was collected in the Benthos sampler. The recovered core length was 72 cm. The core sampling device was capped on both ends, and each end was enclosed in an anaerobic bag. The core was then transported to the Montana Tech Metallurgical Engineering laboratory for sample retrieval.

Core Three—Core Three was collected in the Benthos sampler adapted with a 20-kilogram (kg) collar so the sampler would penetrate deeper into the sediment layer. The recovered core length was 86 cm. The core sampling device was capped on both ends, and each end was enclosed in an anaerobic bag. The core was then transported to the Montana Tech Metallurgical Engineering Laboratory for sample retrieval.

3.3.2 Sample Identification and Sample Handling

Water and core samples were transferred to an argon atmosphere prior to subsequent sample subdividing. Water samples were sealed under argon, and core samples were segmented into subsamples and stored in argon filled containers. All samples were subsequently stored at 4 °C until retrieved for analysis.

Sample Identification

The sample identification logging notation is summarized in Table 3-1.

Sample Handling

Core One—The Core One collection tube (polycarbonate) containing the sediment sample was slid into an argon filled glove box through an O-ring penetration slot in the bottom of the glove box. Argon was continuously admitted into the glove box before the anaerobic bag was withdrawn from the top of the collection tube. The bottom of the collection tube was placed in an O-ring-sealed base plate that was connected to a hydraulic lifter. The anaerobic bag was removed from the top of the collection tube. A polycarbonate ring (5 cm tall) was placed on the top of the collection tube. The core column was raised by the hydraulic lift to the top of the calibrated ring. Water was suctioned off the top of the tube using a 40-cubic centimeter (cc) syringe. The water was removed by this method until the water level in the calibrated tube was decreased 5 cm. The water removed by this technique was placed in a 20-cc centrifuge tube and capped. The remaining water was archived in a glass storage vessel under an argon atmosphere. This procedure was continued until the sediment interface was reached. The sediment was forced into the calibrated ring, and a section pan was forced between the ring and the collection tube top. The 5-cm sample was then lifted off the top of the collection tube, and the calibrated ring was removed leaving the sediment sample on the sectioning pan. The sediment in the upper portion of the collection tube was semi-solid. A portion of the sample was suctioned into a syringe and placed into a centrifuge tube. The remainder was archived. As sampling progressed downward, the sediment became solid enough to hold its shape after sectioning. In this case the sediment was sectioned along its vertical axis into four approximately equal sections. One section (samples BPD-C1-CS1 to CS10) was transferred to a centrifuge tube, and the rest were archived as described above.

The centrifuge tubes were removed from the glove box and subjected to centrifuging (at 20,000 revolutions per minute (rpm) for 15 minutes) to

separate the pore water and the sediment solids. The centrifuged water and solids were separated (in an argon glove box), and the samples were prepared for solution and solid analyses. The solutions were preserved according to the requirements of the QAPP, and the solids were dried at room temperature to constant weight then digested and analyzed by ICP. Pore water and solid sample analysis analytical results are summarized in Section 4; detailed analytical results are presented in Appendix B. X-ray diffraction, SEM, and EDX analyses are summarized in Section 4; additional XRD results are presented in Appendix C. Sample identification descriptions are presented in Table 3-2; a sequence of photographs depicting the sampling sequence is presented in Appendix A.

Chemical characterization of the sediment solids was performed using EPA SW-846 (Method 3052A) digestions (in triplicate). The waters and digestates were analyzed by SW-846 (Method 6010A) using an ICP emission spectrometer.

Core Two—The Core Two collection tube (polycarbonate) containing the sediment sample was slid into an argon filled glove box through an O-ring penetration slot in the bottom of the glove box. Argon was continuously admitted to the glove box before the anaerobic bag was withdrawn from the top of the collection tube. The bottom of the collection tube was placed in an O-ring-sealed base plate that was connected to a hydraulic lifter. The anaerobic bag was removed from the top of the collection tube. A polycarbonate ring (2 cm tall or 5 cm tall) was placed on the top of the collection tube. The core column was raised by the hydraulic lift to the top of the calibrated ring. Water was suctioned off the top of the tube using a 40-cc syringe. The water was removed by this method until the water level in the calibrated tube was decreased 2 cm. The water removed by this technique was placed in a 20-cc centrifuge tube and capped. The remaining water was archived in a glass storage vessel under an argon atmosphere. This procedure continued until the sediment interface was reached. The sediment was forced up into the calibrated ring, and a section pan was forced between the ring and the collection tube top. The 2-cm sample was then lifted off the top of the collection tube, and the calibrated ring was removed leaving the sediment sample on the sectioning pan. The sediment in the upper portion of the collection tube was a semi-solid. A portion of several of the samples was suctioned into a syringe and placed into a centrifuge tube. The remainder was archived. As sampling progressed downward, the sediment became solid enough to hold its shape after sectioning. In this case, the sediment was sectioned along its vertical axis into four approximately equal pie-like sections. One section (samples BPD-C2-CS1, CS2, CS3, CS4, CS5, CS7, CS11, and CS14) was transferred to a centrifuge tube, and the rest were archived as described above.

The centrifuge tubes were removed from the glove box and were subjected to centrifuging to separate the pore water and sediment solids. The centrifuged water and solids were separated (in an argon glove box), and the samples were prepared for solution and solid analyses. The solutions were preserved according to the requirements of the QAPP, and the solids were dried at room temperature to a constant weight then digested and analyzed by ICP. Pore water and solid sample analysis analytical results are summarized in Section 4; detailed analytical results are presented in Appendix B. X-ray diffraction, SEM, and EDX analyses are summarized in Section 4; additional XRD results are presented in Appendix C. Sample identification descriptions are presented in
Table 3-3.

Core Three—The Core Three collection tube (polycarbonate) containing the sediment sample was slid into an argon filled glove box through an O-ring penetration slot in the bottom of the glove box. Argon was continuously admitted to the

glove box before the anaerobic bag was withdrawn from the top of the collection tube.

The bottom of the collection tube was placed in an O-ring-sealed base plate that was connected to a hydraulic lifter. The anaerobic bag was removed from the top of the collection tube. A polycarbonate ring (5 cm or 10 cm tall) was placed on the top of the collection tube. The core column was raised by the hydraulic lift to the top of the calibrated ring. Essentially no water was present on top of the collection tube; therefore, the initial sectioning was performed on the sediment. The sediment was forced up into the calibrated ring, and a section pan was forced between the ring and the collection tube top. The sample was then lifted off the top of the collection tube, and the calibrated ring was removed leaving the sediment sample on the sectioning pan. The sediment in the upper portion of the collection tube was solid enough so that the sectioned sample formed a stable cylinder. The sediment was sectioned along its vertical axis into four approximately equal pie-like sections. One section [samples BPD-C3-CS1(top), CS6(middle), and CS10(bottom)] was transferred to a centrifuge tube, and the rest were archived as described above.

The centrifuge tubes were removed from the glove box and subjected to centrifuging to separate the pore water and sediment solids. The centrifuged water and solids were separated (in an argon glove box), and the samples were prepared for solution and solid analyses. The solutions were preserved according to the requirements of the QAAP, and the solids were dried at room temperature to a constant weight then digested and analyzed by ICP. Pore water and solid sample analysis analytical results are summarized in Section 4; detailed analytical results are presented in Appendix B. X-ray diffraction, SEM, and EDX analyses are summarized in Section 4; additional XRD results are presented in Appendix C. Sample identification descriptions are presented in Table 3-4.

Table 3-1. Sample Identification

Sampling Event	Solution Samples from NISKEN Sampler	Solution and Solid Samples from Benthos Core Sampler	Description
November 18, 1997	VS-1-111897-x (VS=Vertical Sampler-sampler number-date-analytical sample number.)	CS-1-111897-x (CS=Core Sampler-date-analytical sample number.)	Retrieved approximately 2 L of water from the 600-ft level. Retrieved only small amount of surface sediment.
November 20, 1997	VS-1-112097-x (VS=Vertical Sampler-sampler number-date-analytical sample number.)	CS-1-112097-x (CS=Core Sampler-date-analytical sample number.)	Retrieved approximately 2 L of water from the 700-ft level. Retrieved only small amount of surface sediment.
April 22, 1998	BPD-1-x (BPD=Berkeley Pit Deep NISKEN vertical sampler number-analytical sample number.)	BPD-Cx-CSx-x (Berkeley Pit Deep Core number-core slice number-analytical number.)	Retrieved approximately 4 L of water from the 717-ft level. Retrieved (using a Benthos core sampling device) a 70 cm sediment core sample from 717-ft depth; designated as core one.
April 23, 1998		BPD-Cx-CSx-x (Berkeley Pit Deep Core number-core slice number-analytical number.)	Retrieved (using a Benthos core sampling device) a 72-cm and an 86-cm sediment core sample; designated as Cores Two and Three, respectively.

Table 3-2. Sample Sections for Core One

Sample Number	Slice Number	Slice Depth, cm	Depth into Core, cm
BPD-C1-CS1	1	5	5
BPD-C1-CS2	2	5	10
BPD-C1-CS3	3	5	15
BPD-C1-CS4	4	5	20
BPD-C1-CS5	5	5	25
BPD-C1-CS6	6	10	35
BPD-C1-CS7	7	10	45
BPD-C1-CS8	8	5	50
BPD-C1-CS9	9	5	55
BPD-C1-CS10	10	5	60

Note: All samples were reddish in color.

Table 3-3. Sample Sections for Core Two (Photograph Presented in Appendix A)

Sample Number	Slice Number	Slice Depth, cm	Depth into Core, cm
BPD-C2-CS1	1	2	2
BPD-C2-CS2	2	2	4
BPD-C2-CS3	3	2	6
BPD-C2-CS4	4	2	8
BPD-C2-CS5	5	2	10
BPD-C2-CS6	6	8	18
BPD-C2-CS7	7	2	20
BPD-C2-CS8	8	10	30
BPD-C2-CS9	9	10	40
BPD-C2-CS10	10	5	45
BPD-C2-CS11	11	2	47
BPD-C2-CS12	12	10	57
BPD-C2-CS13	13	10	67
BPD-C2-CS14	14	5	72

Note: The core sediment sample was definitely redder in color above 20 cm (from the top) than below. Another change in color occurred below 45 cm. The color was definitely grayer below this interface.

Table 3-4. Sample Sections for Core Three (Photograph Presented in Appendix A)

Sample Number	Slice Number	Slice Depth, cm	Depth into Core, cm
BPD-C3-CS1	1	5	5
BPD-C3-CS2	2	10	15
BPD-C3-CS3	3	10	25
BPD-C3-CS4	4	10	35
BPD-C3-CS5	5	10	45
BPD-C3-CS6	6	5	50
BPD-C3-CS7	7	10	60
BPD-C3-CS8	8	10	70
BPD-C3-CS9	9	10	80
BPD-C3-CS10	10	5	85
BPD-C3-CS11	11	1	86

Note: This core material was a gray, light brown material. Core Three was a different color than Cores One and Two.

4. Presentation and Discussion of Results

The experimental results are presented in Section 4.1 and are discussed in Section 4.2. This experimental test program was conducted at Montana Tech and was directed by Drs. L.G. Twidwell (Department of Metallurgical Engineering), C.A. Young (Department of Metallurgical Engineering), and R.B. Berg (MBMG). The graduate student who assisted the test program was Mr. R. J. Ziolkowski (Department of Metallurgical Engineering).

4.1 Presentation of Results

4.1.1 Deep Water Chemical Composition and Water Properties

The chemical composition of Berkeley Pit water at various depths and various deep water positions is presented in Table 4-1. The 600-, 700-, and 717-ft samples were collected at the water/sediment interface. The anion concentrations for chloride, fluoride, nitrate, nitrite, phosphate, and sulfate as a function of depth are presented in Table 4-2 (May 5, 6, and 7, 1998 water sampling event). Iron speciation data as a function of depth is presented in Table 4-3 (May 5, 6, and 7, 1998 water sampling event). The dissolved oxygen (DO), oxidation-reduction potential (E_H), pH, temperature, and turbidity in situ values as a function of depth are presented in Table 4-4 (May 5, 6, and 7, 1998, sampling event). A detailed description and discussion of the characteristics of the water column are presented in Reference 8.

A discussion of the above results is presented in Section 4.2.1.

4.1.2 Pore Water Characterization

4.1.2.1 Pore Water Chemical Analyses

The associated water in the sediment was separated as described in Section 3.3.2. The separated water was split into two fractions, i.e., one fraction was used to determine elemental concentrations; the second fraction was preserved with hydrochloric acid, and iron speciation was performed.

A summary of the pore water analytical results are presented in Tables 4-5 to 4-8.

4.1.2.2 Iron Speciation in Pore Water

The iron speciation in pore waters separated from Cores One, Two and Three are presented in Table 4-9.

4.1.2.3 Properties of Pore Water

The pH, solution potential, and DO in Cores One, Two, and Three are presented in Table 4-10.

A discussion of the above results is presented in Section 4.2.2.

4.1.3 Sediment Solids Characterization

4.1.3.1 Solids Composition

4.1.3.1.1 Deep Water Sediment Surface Solids

The chemical composition of the sediment surface solids retrieved during the November 18, 1997, (600 ft) and November 20, 1997, (700 ft) and April 22, 1997, (717 ft) sampling events are summarized in Table 4-11. The samples collected during the November sampling event were surface sediment samples, i.e., cores were not retrieved. The April 22 sample was an intact core sample that had 10 cm of water on top of the sediment, i.e., the reported data in Table 4-11 are for the solids suspended in the 10 cm of water.

4.2.5.1.2 Core Analyses

The chemical composition of selected solid samples from the three cores retrieved during the April 22 and 23, 1997, (717 ft) sampling events are summarized in Tables 4-12 (Core One), 4-13 (Core Two and Core Three).

4.1.3.1.3 Sediment Solids Content

The sediment solids content for each core as a function of depth is presented in Table 4-14.

4.1.3.2 Solids Characterization

Solids characterization studies included structure determinations, XRD, optical microscopy, and SEM-EDX**.**

4.1.3.2.1 X-Ray Diffraction and Petrographic Studies

X-ray diffraction studies and petrographic studies were conducted on selected solid samples.

X-Ray Diffraction

X-ray diffraction studies were conducted on many of the core segments. Example patterns for two widely different core slices are presented in Figures 4-1 (sediment/deep water interface), and 4-2 (deepest sediment sample). An overlay of the two patterns is pictured in Figure 4-3. The investigated solid core samples all included the major phases: quartz, jarosite (perhaps a mixture of potassium and hydrogen jarosites), biotite, and gypsum. An estimation of the relative amounts of each phase (compared to quartz) is presented in Table 4-15. Two (Core Two, top and Core Three bottom) sediment sample solids were separated into +325 mesh [+44 micrometers (μm)] and -325 mesh (-44 μm) fractions. These fractions were also subjected to XRD evaluation. The patterns are presented in Appendix C. The patterns demonstrate that the jarosite particulate phase is finely divided and is concentrated into the -325 mesh fraction. This is in agreement with the petrographic analysis of Berg who estimated that the jarosite phase particulate size is less than 2 μm .

The experimental results are discussed in Section 4.2.5.2.

Petrographic Study of Sediment/Deep Water Interface Solids

Petrographic examinations of the 600 ft and 700 ft (fall 1997) and Robins 700 ft (spring 1995) samples were performed.[2] The mineralogy of these three samples (all sediment/deep water interface samples) was similar; the only difference was in the relative proportion of the individual minerals. Minerals in the samples consisted of a detrital component (native material) derived from veins, alteration envelopes, and granitic country rock exposed in the walls of the Berkeley Pit and a precipitated component that consisted of those minerals directly precipitated from the water in the Pit. The mineralogy results are summarized in Table 4-16. A summary of observations is presented in Table 4-17. All three samples were checked for calcite under the binocular microscope using dilute hydrochloric acid. Calcite was not detected by this very sensitive technique.

The petrographic study results confirmed the XRD study results with respect to the presence of the major components, i.e., quartz, biotite, jarosite, and gypsum.

Petrographic Study of Core Solids

Petrographic examinations of samples from Cores Two and Three were performed. Samples were prepared from position slices from each core as a function of depth from the top of each core. The mineralogy of the samples was similar; the only difference was in the relative proportion of the individual minerals. The results of this study were in agreement with the descriptions presented above for the 600- and 700-ft samples, i.e., the examinations showed that minerals in the samples consisted of a detrital component (native material) derived from veins, alteration envelopes and granitic country rock exposed in the walls of the Berkeley Pit, and a precipitated component that consisted of the minerals directly precipitated from the water in the Pit. A summary of the observed mineralogy in Core Two and Core Three samples is presented in Table 4-18. Observations of particle size and shape are presented in Table 4-19.

4.1.3.2.2 Microscopic Chemical Analysis Studies

Microscopic chemical analyses of particles in several sediment solids were determined using SEM-EDX. The samples were scanned with the SEM to locate individual particles. The bulk chemistry of the conglomerate was determined by collected data on a relatively large portion of the sediment solid particles. Individual particles were then identified, and spot analyses were taken.

Particle Identification in Sediment Surface Sample and Cores Two and Three

Several specific individual particles were identified in the sediment-surface solid sample (600 ft) in Core Two, slice one (top of Core Two) and slice eleven (bottom of Core Two); and in Core Three, slice ten (deepest sediment sample collected). The results are summarized in Table 4-20.

The SEM study showed the presence of a relatively large amount of very fine jarosite particulates. The jarosite was evident on essentially all the larger particle surfaces. The EDX study was directed toward spot analyses on individual mineral particles. All the samples showed the presence of the same phases, only the relative amounts varied. Detrital particles and precipitated particles were identified. The native particles included biotite, plagioclase, and quartz. The precipitated particles included jarosite and gypsum.

The SEM study showed the presence of a relatively large amount of very fine jarosite particulates. The jarosite was evident on essentially all the larger particle surfaces. The EDX study was directed toward spot analyses on individual mineral particles. All the samples showed the presence of the same phases; only the relative amounts varied. Detrital particles and precipitated particles were identified. The native particles included biotite, plagioclase, biotite and quartz. The precipitated particles included jarosite and gypsum

4.1.3.2.3. Magnetic Fraction

A preliminary semiquantitative study was made to separate magnetic material. A strong hand magnet was placed outside a tube positioned at a 45° angle. Solid sample was passed through the tube, and the magnetic fraction was separated. The product from the first pass was passed through the tube a second time. Using this technique, the sediments were found to contain a magnetic component, e.g., BPD-C2 CS1 (top slice) contained 5% magnetic material; BPD-C3-CS10 (deepest sample) contained 6% magnetic material.

4.2 Discussion of Results

4.2.1 Deep Water Data Comments

The water column and deep water experimental data have been presented previously in Section 4.1.1.

There does not appear to be significant differences in the elemental content of the upper water column and the deep water (near sediment) samples. However, iron shows a slight (approximately 5%) increase in concentration with depth (from surface to 715 ft). The ferrous-to-ferric ratio shows a marked increase from the surface to about 100 ft, then the ratio remains approximately constant from 100 to 715 ft, i.e., the ferrous concentration increased steadily from approximately 240 ppm at 2 ft to approximately 730 ppm at 100 ft then remained relatively constant to 715 ft. The ferric concentration dropped from approximately 690 ppm at 2 ft to approximately 300 ppm at 100 ft then remained relatively constant to 715 ft. These effects are illustrated in Figure 4-4 (Ref. 8).

Phosphate, nitrate, and nitrite concentrations were found to be less than the detection limit at all depths. Fluoride (approximately 30 to 40 ppm) and chloride (approximately 10 to 15 ppm)

concentrations were relatively constant with depth. Sulfate showed an increasing concentration as a function of depth, e.g., 8.7 g/L at 2 ft and 9.5 g/L at 888 ft.

The in situ measured DO concentration was relatively high near the surface; it then dropped dramatically from 2 to 18 ft then rose to levels exceeding the level near the surface. The DO concentration then became relatively constant with increasing depth from approximately 100 ft to near the sediment surface. The data appears to suggest that surface water turnover may have occurred down to the 100-ft level. The collection of additional data is required to confirm this preliminary conclusion.

The conclusion that the oxygen content is not significantly lower in the deep water than in the water column is an important finding because it was suspected that the solution conditions would become more reducing with depth. The solution E_H data supports the conclusion that the water does not become appreciably more reducing with depth, i.e., a decrease in the solution potential of only approximately 40 millivolts (mV) 10% was measured over a depth of approximately 20 ft; then the solution potential remained essentially constant to near the sediment surface. The potential/pH diagram for Berkeley Pit water is presented in Figure 4-5. Data points for water and sediment/pore water samples are superimposed on the diagram. Note that the diagram illustrates jarosite should form (and does form as discussed in subsequent sections) for the conditions present in the Pit lake water system. The diagram also illustrates that the solution E_H/pH conditions in the Pit lake water are near the jarosite/schwertmannite boundary; therefore, there may be some schwertmannite formation in the water column.

Additional characterization of the water column is presented and discussed in References 8 and 9.

4.2.2 Pore Water Data Trends

The water column and deep water experimental data are presented in Section 4.1.2.

The pore waters were not less contaminated than the deep waters. A comparison of shallow, deep and pore water in the deepest sediment sample (Core Three, slice ten, BPD-C3-CS10) is presented in Table 4-21. The shallow and deep waters have similar elemental concentrations. The pore water has a lower concentration of arsenic, potassium, phosphorus, and sulfur; and it has a higher concentration of copper and iron.

Iron Content

The iron concentration data in the pore water is quite surprising. The total iron content in the deep water just above the sediment is approximately one-half of what it is in the pore water at the top of the sediment. This is a real effect because the ICP data for total iron and the spectrophotometric data are in relatively good agreement, i.e., two independent analyses confirm one another. The abrupt change in the iron content is demonstrated graphically in Figure 4-6. Note that the ferrous specie predominates in the sediment pore waters; it is approximately twice the concentration in the deep water just above it but it drops off in concentration with depth into the core. A dicussion of these results is presented in Section 4.2.4.

Iron complexation in the deep water samples and in the pore water samples were determined by using the chemical equilibrium program, STABCAL, developed by Dr. H. Huang at Montana Tech (Ref. 10). The results show that the speciation of iron in the solution phases is primarily Fe^{+2} and $FeSO_4$E. The major iron (+3) species (present only in a relatively low concentration) is $FeSO_4^{+1}$. The complexation speciation results are presented in Figure 4-7 (comparison of deep water with core water) and Figure 4-8 (comparison of pore waters).

The zero point of charge has been determined for the sediment solids, and the result is presented graphically in Figure 4-9.

4.2.3 Solids Characterization Comments and Summary

The sediment experimental data is presented in Section 4.1.3.

The three cores show the same general elemental composition versus depth trend, i.e., arsenic, iron, potassium, and sulfur show a decreasing trend with depth. These results are shown in graphical form in Figures 4-10 through 4-12.

4.2.4 Ferrous Concentration in Pore Waters

It was noted in Section 4.1.2 that the ferrous concentration in the sediment surface layers was greatly elevated over the concentration in the deep water above the sediment. The abrupt increase in the ferrous concentration in the upper surface layers of the sediment can be explained as follows. The major iron-bearing compound in the sediment surface is potassium jarosite. Jarosite contains iron in the ferric valence state. Therefore, a reduction reaction must be occuring to form the elevated concentrations of ferrous present.

Jonas (Ref. 8) experimentally found that the sediment contains 0.3 to 0.4% organic carbon. The origin of this carbon is presently unknown but could be from timbers, oils, settled biological debris, etc..

The present speculation is that the organic carbon reacts with jarosite according to the following reaction:

$$4\ KFe_3(SO_4)_2(OH)_6 + 9\ H^+ + 3\ C(organic) = 3\ HCO_3^{-1} + 12\ Fe^{+2} + 8\ SO_4^{-2} + 15\ H_2O + 4\ K^+ \qquad [4\text{-}1]$$

Using the elemental concentrations and pH conditions (as an example) that exist in the upper layer of Core One, the free energy of reaction can be calculated for the resident conditions. The calculational procedure involves determining the activities for each of the species included in the reaction by using the STABCAL software then solving for the free energy of reaction for the resident conditions. The free energy of reaction equation is presented below in Equation [4-3].

? GE = -RT Ln K (Standard Free Energy of Reaction)
$= \Sigma G E_{products} - \Sigma G E_{reactants}$ [4-2]

? G = RT Ln [Q/K] (Free Energy of Reaction) [4-3]

where:

R=1.987 calories/g/mole (M) K
T=298.15EK
K=Equilibrium constant calculated from the standard free energy of reaction.
Q=Reaction quotient (from resident elemental activites) calculated from the measured solution conditions.

If ? G is negative, then the reaction is thermodynamically possible.

An example calculation is presented below for Core One top slice conditons.

Conditions in Pore Water (BPD-C1-CS1)
(Table 4-22)

Speciation
The equilibrium calculational software STABCAL was used to determine the elemental speciation of the above experimental data. The results are presented in Table 4-23.

Determination of K
The equilibrium constant K, for the reaction [4-1] can be determined from equation [4-2]:

$4\ KFe_3(SO_4)_2(OH)_6 + 9\ H^+ + 3\ C(organic) = 3\ HCO_3^{-1} + 12\ Fe^{+2} + 8SO_4^{-2} + 15\ H_2O + 4\ K^+$ [4-1]

? GE =-RT Ln K (Standard Free Energy of Reaction)=
$\Sigma G E_{products} - \Sigma G E_{reactants}$ [4-2]

? GE= 3[3? GE(HCO_3^{-1})+12? GE(Fe^{+2}) + 8? GE(SO_4^{-2})
+ 15? GE(H_2O) + 4? GE(K^+)]

-3[4? GE($KFe_3(SO_4)_2(OH)_6$)]

=3(-140.24 kcal/mole)+12(-18.86)+8(-177.95)
+15(-56.675)+4(-67.70)-4(-787.07)

=-43.3 kcal=-RTLnK=-(0.001987)(298.15)LnK

K=5.7E31

Determination of Q

The reaction quotient, Q, for the reaction [4-1] can be determined from experimental results presented in Table F-2:

$Q=a(HCO_3^{-1})^3a(Fe^{+2})^{12}a(SO_4^{-2})^8a(K^+)^4]/\ a(C_{organic})^3a(H^+)^9$,

where a= activities

The activity of the organic carbon is estimated to be equivalent to the mole fraction of carbon in the solid phase, a(C)=N(C)=0.019.

$Q=(1.74E-04)^3(7.08E-03)^{12}(7.44E-05)^4/(0.019)^3(8.0E-04)^9$

=7.1E-36

Determination of Free Energy of Reaction, ?G

The Free Energy of Reaction can be determined from Equation [4-3]

? G = RT Ln [Q/K] (Free Energy of Reaction) [4-3]

=(1.987)(298.15)Ln[7.1E-36/5.7E31]
=-91.3 kilocalorie (kcal)

Note that the free energy of reaction indicates a favorable reaction. Therefore, the ferrous concentration in the pore waters is likely controlled by the rate at which jarosite (or other ferric compounds, such as schwertzmannite) is reduced.

4.2.5 Modeling

The concentration of many of the individual elements in the pore water can likely be explained by modeling the solubility of various compounds known to be present in the sediment solids. The modeling effort for this project was initiated. Further modeling results will be forthcoming as a part of the Master of Science thesis being prepared by Mr. R. J. Ziolkowski (Ref. 6). The modeling results presented in the following sections are considered to be preliminary and more detailed considerations of the experimental data may alter the final conclusions.

The equilibrium concentration/pH diagrams presented in the following figures have been prepared using the software program STABCAL developed by Dr. H.H. Huang (Ref.10). This program requires standard free energy of formation data for all species present in the system. The data used in this modeling effort were primarily from (MINTEQ) (Ref. 11).

X-ray diffraction analysis and petrographic evaluation of the sediments have shown the presence of quartz, muscovite, jarosite, and gypsum. Other mineral phases are present in the sediment, however, a complete evaluation and identification has not been completed at this time.

Aluminum

Aluminum is saturated in the core pore waters (see Figure 4-13). The likely compound controlling the aluminum concentration in the sediment is muscovite ($KAl_3Si_3O_{10}(OH)_2$). However, muscovite solubility does not appear to explain the aluminum concentration in the water column. The aluminum concentration in the water column is presently unexplained.

Silicon
Silicon appears to be saturated in the water column. The likely compound controlling the solution concentration in the water is silica. This result is presented in Figure 4-14. The implication of this result is that silica is being formed in the water column by precipitation. Therefore, the source of silica in the Berkeley Pit is through precipitation and by the supply of native quartz from the Pit sidewalls. Silicon is also saturated in the sediment pore water. The likely compound controlling the silicon concentration in the sediment pore water is muscovite ($KAl_3Si_3O_{10}(OH)_2$).

Potassium
Potassium is at saturation conditions in the water column and in the sediment pore waters, (see Figure 4-15). The likely compound controlling the potassium concentration in the water column and in the pore waters is potassium jarosite.

Ferric Iron
The ferric iron concentration in both the water column and in the sediment pore water is greater than would be predicted by jarosite formation. The ferric concentration in both the water column and in the core pore waters is likely controlled by the formation of schwertzmannite, i.e., the ferric concentration is likely controlled by the solubility of schwertzmannite. This effect is illustrated in Figure 4-16 for the water column and Figure 4-17 for the core pore waters. There is some question as to whether the thermodynamic free energy of formation for schwertzmannite is well defined.[3] A rigorous redetermination of the free energy of formation of schwertzmannite should be conducted.

The experimental data also fits the ferric concentrations predicted by modeling of the solubility of ferrihydrite. However, the E_H/pH diagram presented previously in Figure 4-5 suggests that ferrihydrite does not form at Berkeley Pit pH acidities. Also, a study by Levy, et al. of the Spenceville Pit in Nevada (a pit that has a similar acidity and elemental content) concluded that ferrihydrite was not formed (Ref. 12).

Calcium
The calcium concentration in both the water column and in the sediment pore water is likely to be set by gypsum saturation (see Figure 4-18).

Arsenic
Arsenic is saturated in the core pore waters (see Figure 4-19). The likely compound controlling the arsenic concentration in the sediment is ferrous arsenate ($Fe_3(AsO_4)_2$). Ferrous arsenate solubility however does not appear to explain the arsenic concentration in the water column (Figure 4-20).

As stated above, further modeling work will be performed in an effort to be able to answer several presently unanswered questions, such as:\

- what is the reason for the elevated ferrous concentration in the sediment upper layer pore water?
- why does the copper concentration increase with depth in the pore water?
- what controls the aluminum and arsenic concentration in the water column?

[3] H.H. Huang and L. Twidwell (Montana Tech) personal communication, 1998.

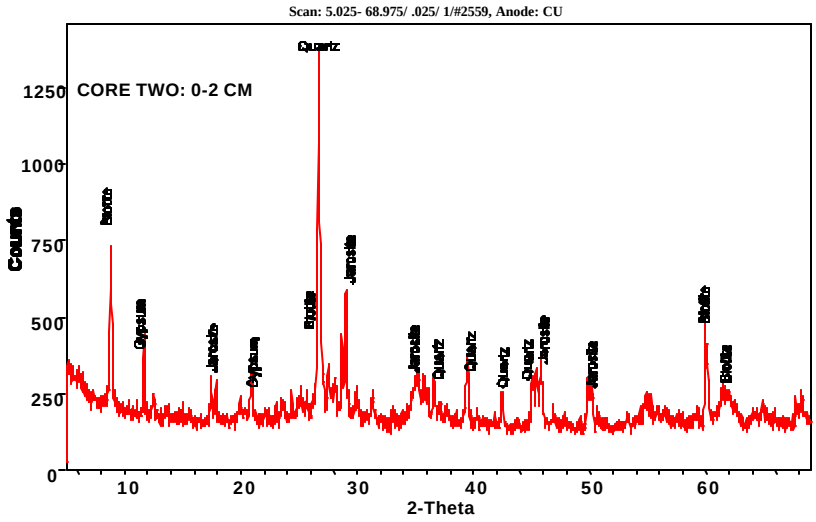

Figure 4-1. X-ray diffraction pattern for the sediment solid surface slice (0 to 2 cm) from Core Two (the peaks labeled biotite are probably the result of the presence of both biotite and muscovite).

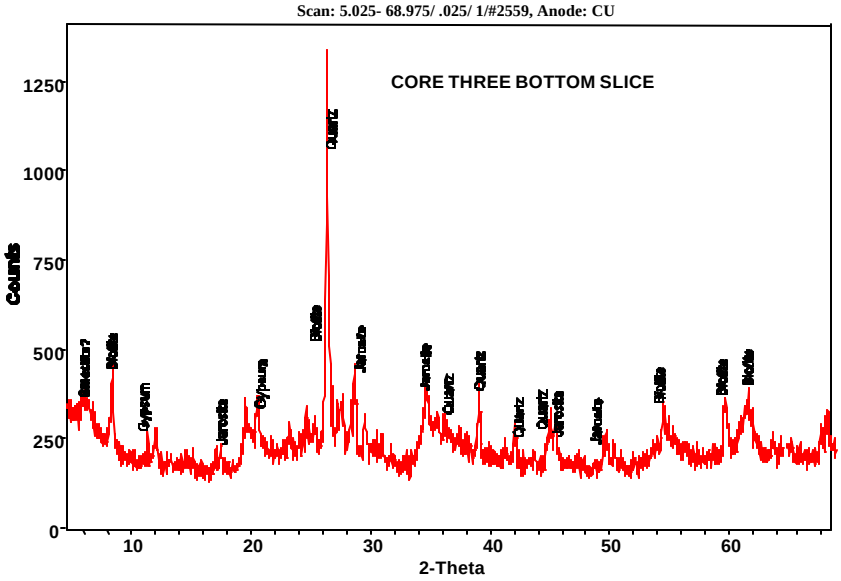

Figure 4-2. X-ray diffraction pattern for the sediment solid bottom slice (75 to 80 cm) from Core Three (the peaks labeled biotite are probably the result of the presence of both biotite and muscovite).

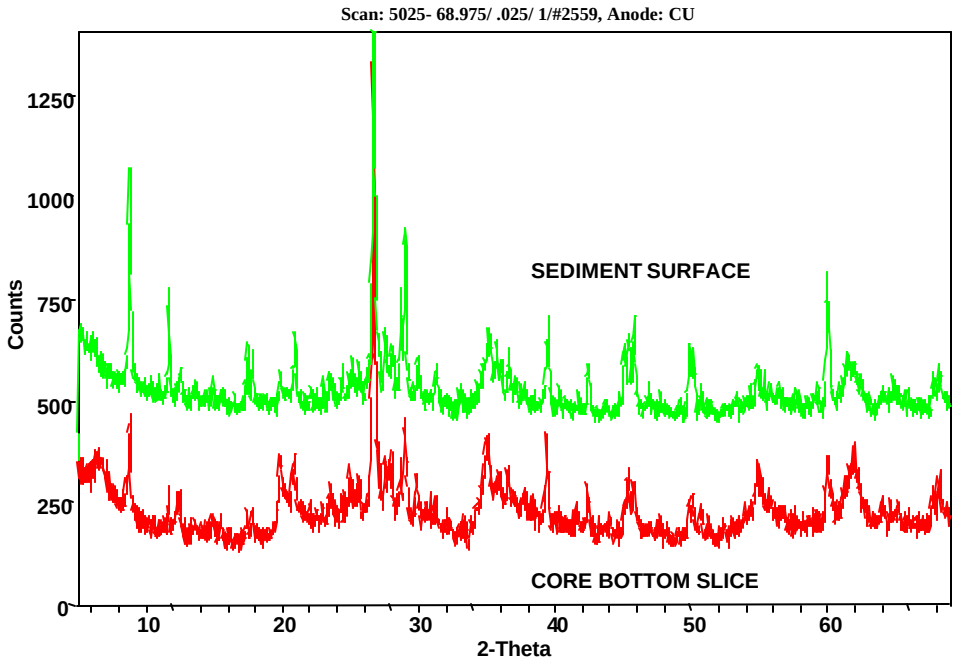

Figure 4-3. X-ray diffraction patterns (superimposed) for the sediment solid surface slice (sediment closest to deep water interface) and the deepest sediment slice (from Core Three).

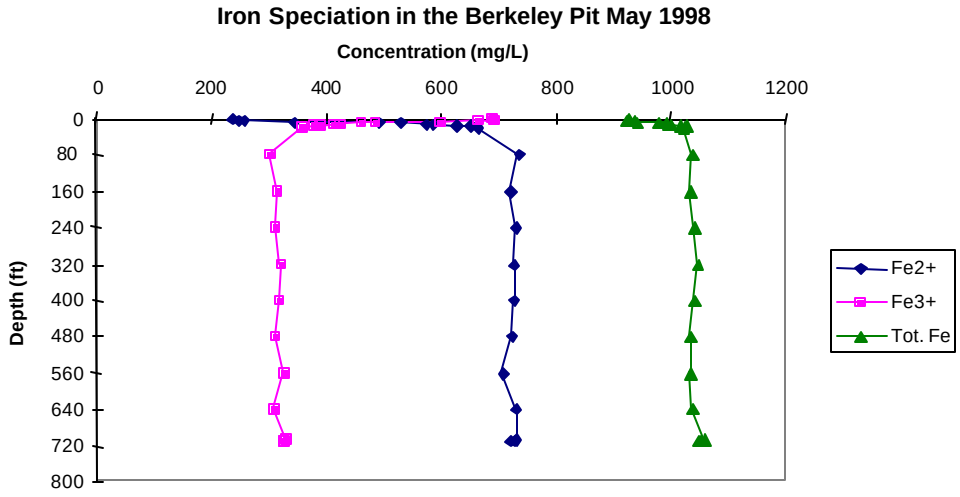

Figure 4-4. Iron speciation as a function of water depth (Ref. 8).

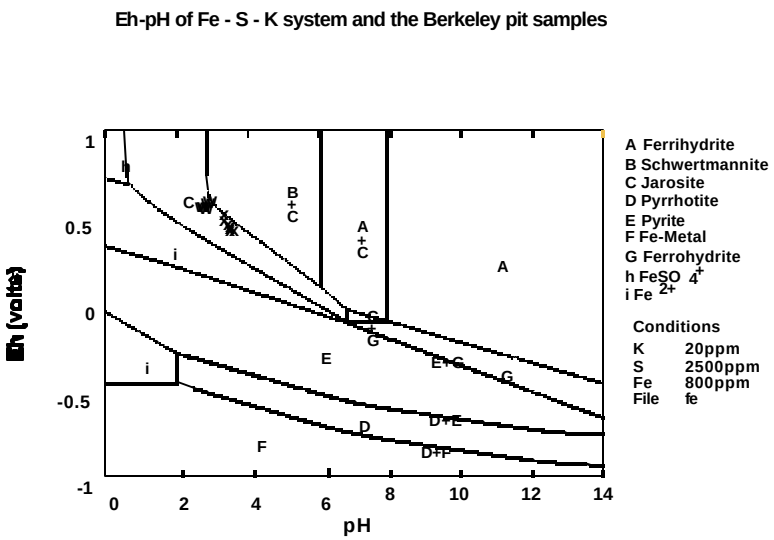

Figure 4-5. E_H/pH diagram for the iron-sulfur-potassium water system at 25 EC (data points for water conditions in the Berkeley Pit are shown using the letter w; data points for pore water conditions in sediments are shown using the letter x).

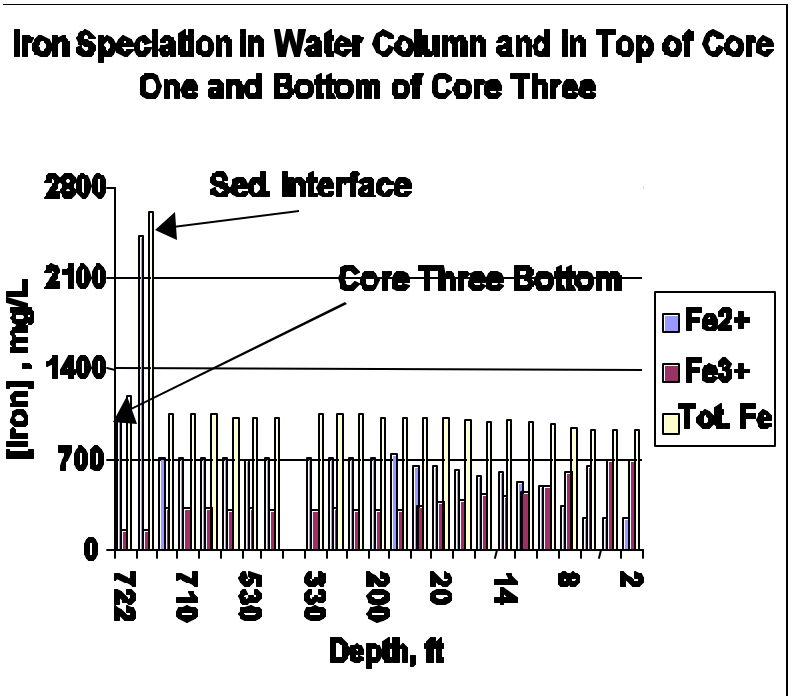

Figure 4-6. Iron speciation in the water column compared to cores one and three.

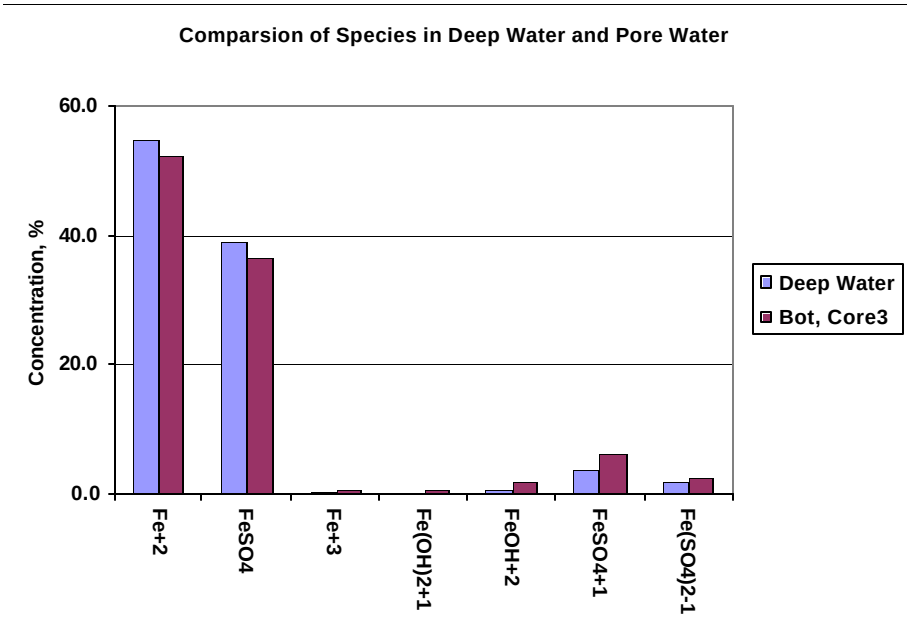

Figure 4-7. Comparison of major iron species present in deep water and in the deepest sediment sample (as predicted by STABCAL).

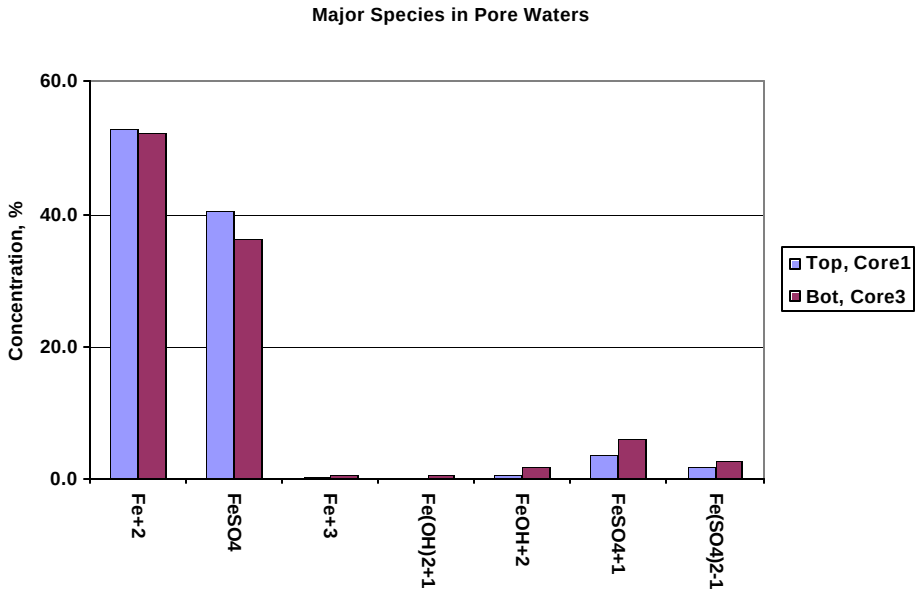

Figure 4-8. Comparison of major iron species present in the sediment surface sample and deepest sediment sample (as predicted by STABCAL).

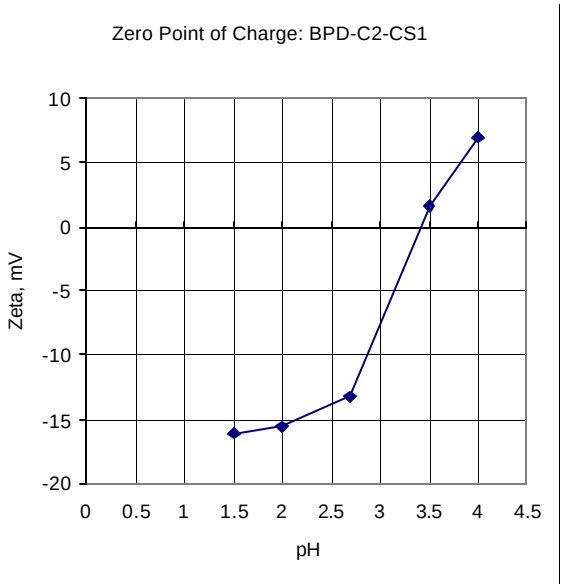

Figure 4-9. Zero point of charge for sediment solids (BPD-C2-CS1).

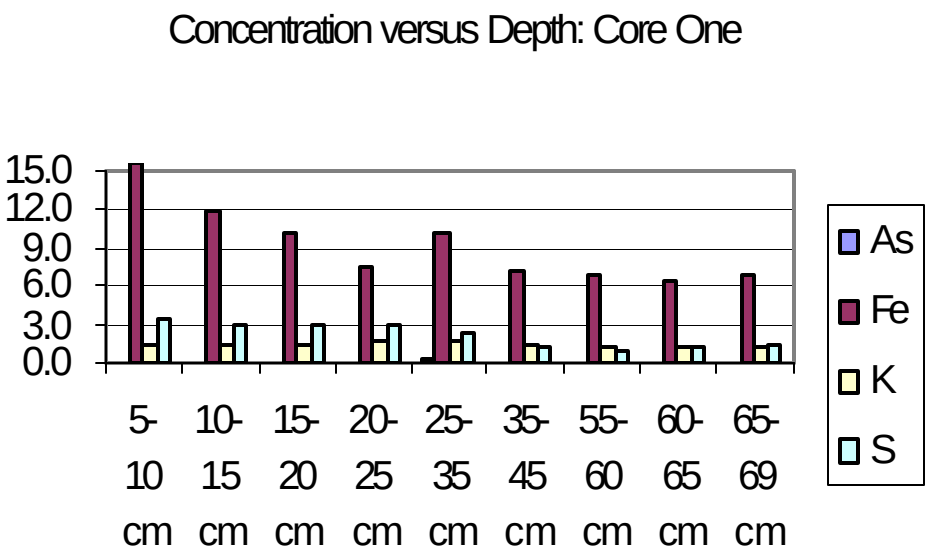

Figure 4-10. Elemental composition of iron, sulfur, potassium, and arsenic versus Core One depth (elements decreased in composition top to bottom: Fe (15.5%-6.8%), S (3.5%-1.3%), K (1.6%-1.2%), As (0.11-0.07%).

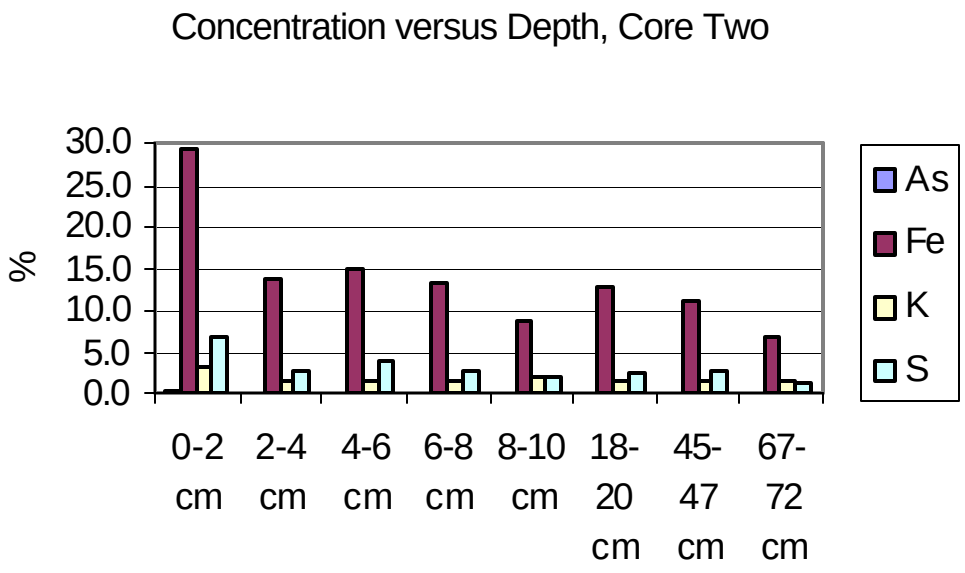

Figure 4-11. Elemental composition of iron, sulfur, potassium, and arsenic versus Core Two depth (elements decreased in composition top to bottom: Fe (29.2%-6.9%), S (6.8%-1.2%), K (3.2%-1.4%), As (0.25-0.07%).

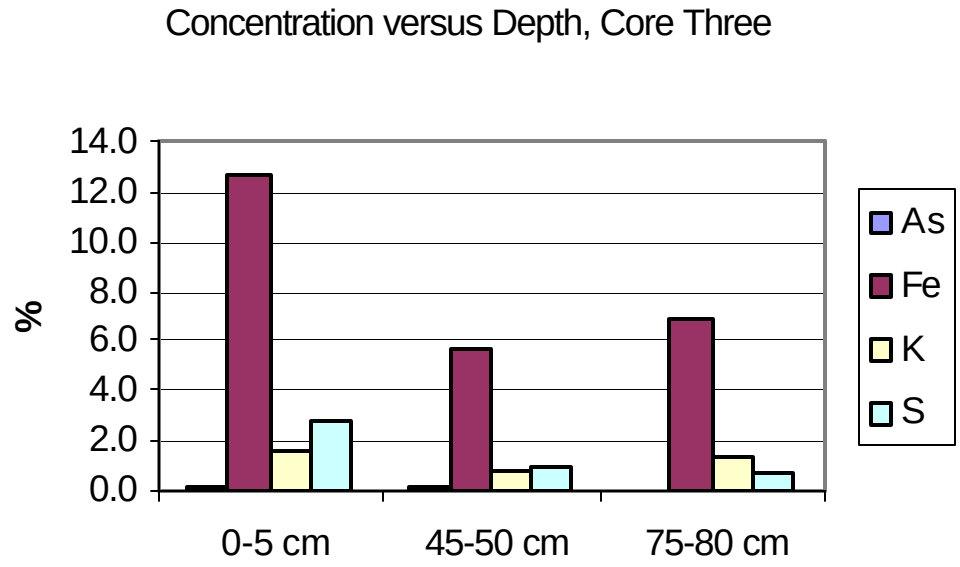

Figure 4-12. Elemental composition of iron, sulfur, potassium, and arsenic versus depth for Core Three (elements decreased in composition top to bottom: Fe (12.6%-6.9%), S (2.8%-0.6%), K (1.6%-1.3%), As (0.09-0.04%).

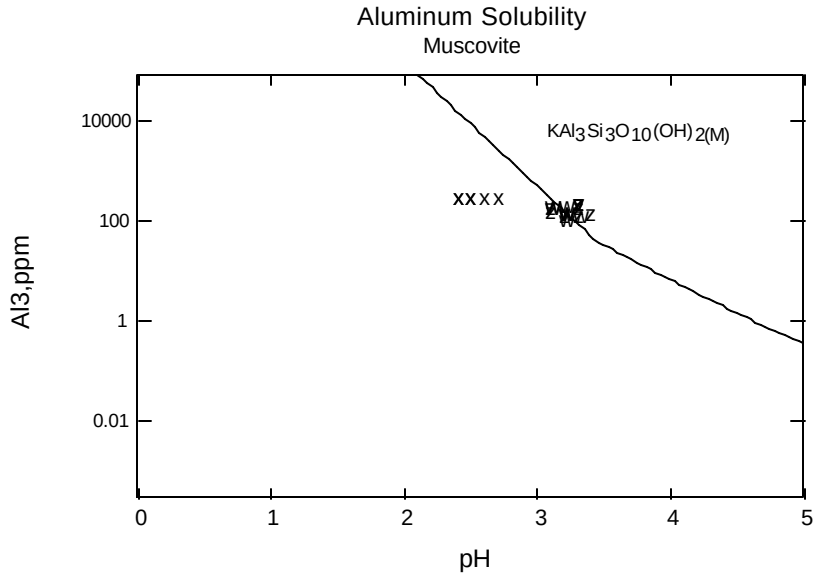

Figure 4-13. Aluminum concentration in Berkeley Pit lake water and solubility in sediment/ pore water (x=water column, z="Core One pore water, w=Core Two pore water, v=Core Three pore water).

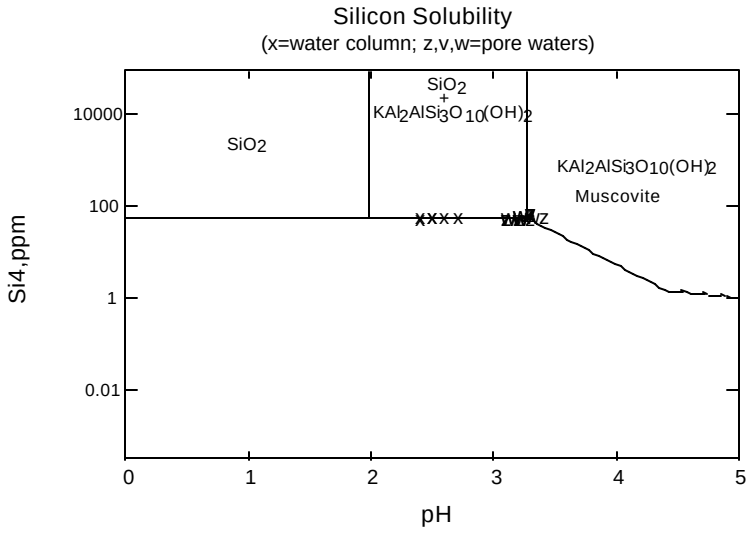

Figure 4-14. Silicon solubility in Berkeley Pit lake water and in sediment/pore water (x=water column, z=Core One pore water, w=Core Two pore water, v=Core Three pore water).

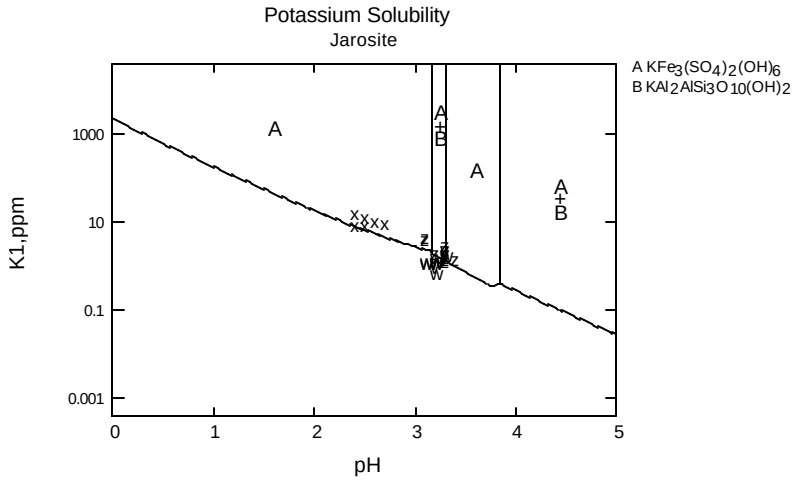

Figure 4-15. Potassium solubility in Berkeley Pit lake water and in sediment/pore water (x=water column, z=Core One pore water, w=Core Two pore water, v=Core Three pore water).

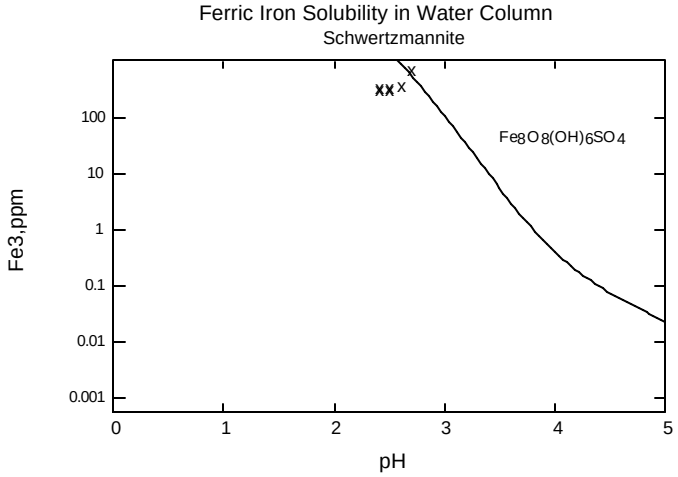

Figure 4-16. Ferric solubility in Berkeley Pit lake water (x=concentration of ferric in water column).

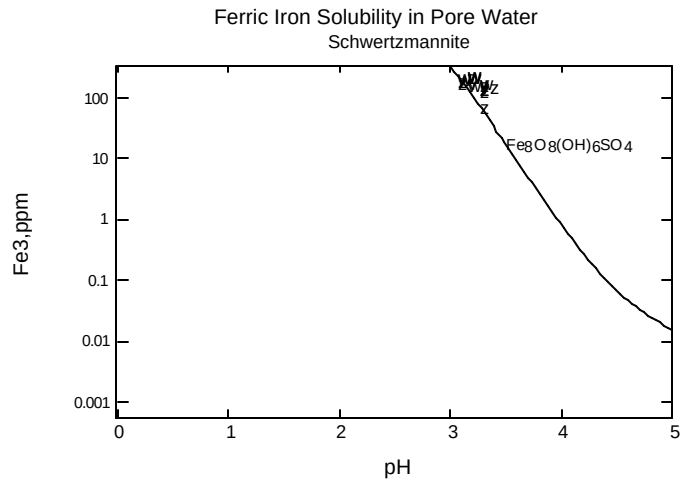

Figure 4-17. Ferric solubility in sediment pore water (z=Core One pore water, w=Core Two pore water, v=Core Three pore water).

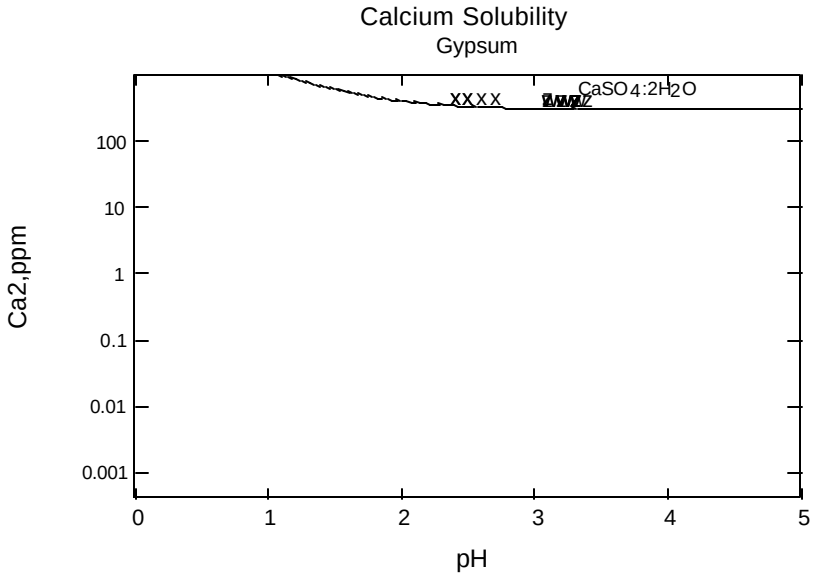

Figure 4-18. Calcium solubility in Berkeley Pit lake water and sediment/pore water (x=water column, z=Core One pore water, w=Core Two pore water, v=Core Three pore water).

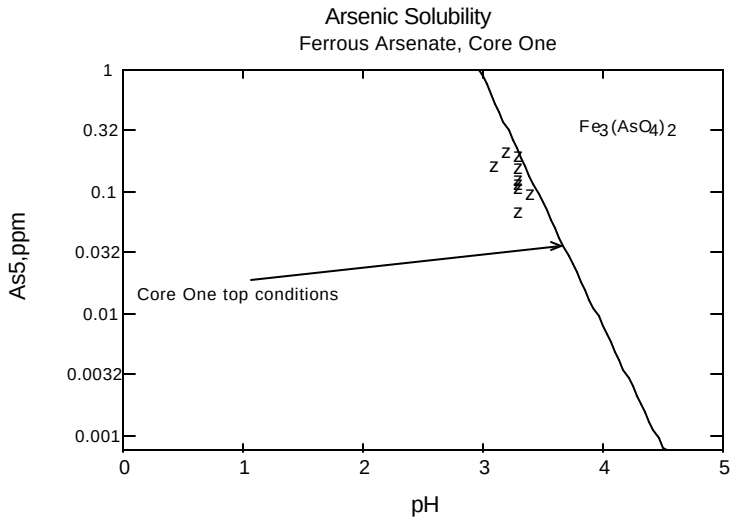

Figure 4-19. Arsenic concentration in Berkeley Pit lake water (x=water column, z=Core One pore water, w=Core Two pore water, v=Core Three pore water).

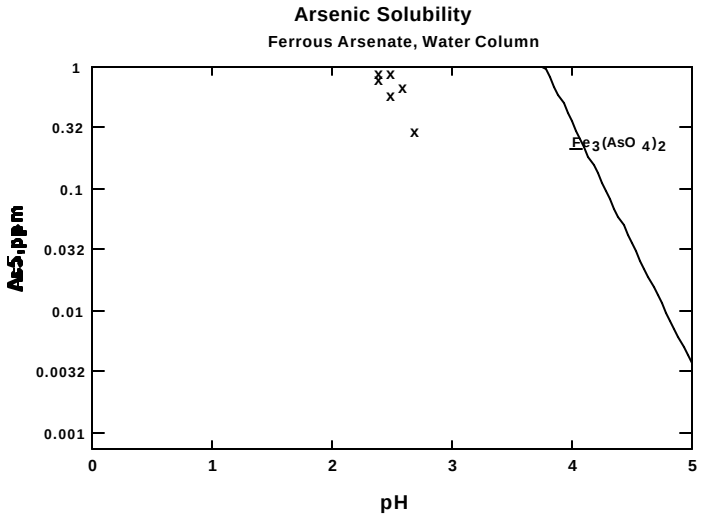

Figure 4-20. Arsenic concentration in Berkeley Pit lake water (x=water column).

Table 4-1. Chemical Composition of Berkeley Pit Lake Water

	Concentration, milligram per Liter (mg/L) (ppm)				
	0 to 25 ft	**50 to 300 ft**	**600 ft**	**700 ft**	**717 ft**
Al	302	295	296	299	293
As	0.3	0.7	0.6	0.8	0.9
Ca	468	462	470	469	477
Cd	2.4	2.3	2.2	2.3	2.4
Cu	212	206	199	194	191
Fe	892	1,088	1,109	1,133	1,097
K	9	10	12	15	8
Mg	526	500	496	494	491
Mn	242	228	231	233	235
Na	116	115	128	123	110
Pb	0.01	0.01	0.10	0.07	0.04
S	2,752	2,743	2,753	2,823	2,825
Si	55	55	56	51	54
Zn	642	628	654	654	646

Note: Upper water column data (0- to 25-ft and 50- to 300-ft depths) are for samples collected May 5, 6, and 7, 1998. The deep water data for 600- and 700-ft depths are for samples collected November 18 and 20, 1997. The deep water data for the 717-ft depth are for samples collected April 22, 1998. Results are the average of triplicate analyses.
All analyses performed by Dr. W. Chatham and his coworkers at the Kelley Mine Analytical Facility.

Table 4-2. Anions in Berkeley Pit Lake Water as a Function of Depth (Ref. 8)

Sample (BPD-sampling depth in ft)	Composition, mg/L (ppm)					
	F^{-1}	Cl^{-1}	NO_2^{-1} as N	NO_3^{-1} as N	PO_4^{-3} as P	SO_4^{-2}
BPD-0.5	34.2	14.5	<DL	<DL	<DL	8,700.2
BPD-01	32.6	12.2	<DL	<DL	<DL	8,896.7
BPD-02	36.7	11.8	<DL	<DL	<DL	8,981.5
BPD-04	33.3	12.9	<DL	<DL	<DL	9,032.7
BPD-06	33.7	15.8	<DL	<DL	<DL	9,167.2
BPD-08	32.5	12.0	<DL	<DL	<DL	9,079.6
BPD-10	32.8	12.1	<DL	<DL	<DL	9,197.6
BPD-12	36.3	15.5	<DL	<DL	<DL	9,139.8
BPD-14	31.9	12.4	<DL	<DL	<DL	8,840.5
BPD-16	35.8	11.8	<DL	<DL	<DL	9,037.2
BPD-18	33.1	10.5	<DL	<DL	<DL	9,159.6
BPD-20	33.0	12.1	<DL	<DL	<DL	9,245.5
BPD-25	36.5	11.7	<DL	<DL	<DL	9,076.2
BPD-50	31.8	11.8	<DL	<DL	<DL	9,118.8
BPD-50A	32.4	10.8	<DL	<DL	<DL	9,174.9
BPD-100	32.3	11.4	<DL	<DL	<DL	9,259.1
BPD-100A	31.3	11.5	<DL	<DL	<DL	9,141.2
BPD-200	36.6	11.3	<DL	<DL	<DL	9,225.9
BPD-227	31.7	10.6	<DL	<DL	<DL	9,229.8
BPD-300	33.6	12.3	<DL	<DL	<DL	9,098.8
BPD-327	36.5	11.2	<DL	<DL	<DL	9,237.3
BPD-427	33.3	10.9	<DL	<DL	<DL	9,202.0
BPD-527	37.5	10.5	<DL	<DL	<DL	9,257.0
BPD-627	32.6	11.6	<DL	<DL	<DL	9,233.4
BPD-707	33.1	12.6	<DL	<DL	<DL	9,331.1
BPD-712	33.3	11.0	<DL	<DL	<DL	9,437.8
BPD-715	37.6	11.3	<DL	<DL	<DL	9,501.1
Instrument Detection Limit	0.053	0.109	0.026	0.034	0.277	0.300

Note: Samples collected May 5, 6, and 7, 1998.
All analyses performed by Dr. W. Chatham and his coworkers at the Kelley Mine Analytical Facility.

Table 4-3. Iron Speciation in Berkeley Pit Lake Water as a Function of Depth (Ref. 8)

Sample (BPD-sampling depth in ft)	Concentration, mg/L (ppm)			
	Fe^{+2}	Fe^{+3}	Total Fe	Fe^{+2}/Fe^{+3}
BPD-2	236.9	689.8	926.7	0.3
BPD-4	244.9	690.6	935.6	0.4
BPD-6	256.9	665.3	922.3	0.4
BPD-8	342.9	597.1	940.0	0.6
BPD-10	492.9	484.8	977.8	1.0
BPD-12	530.9	460.2	991.1	1.2
BPD-14	586.9	413.1	1,000.0	1.4
BPD-16	572.9	422.6	995.5	1.4
BPD-18	626.9	388.6	1,015.5	1.6
BPD-20	650.9	377.9	1,028.8	1.7
BPD-25	664.9	357.3	1,022.2	1.9
BPD-100	734.9	302.8	1,037.7	2.4
BPD-200	720.9	314.6	1,035.5	2.3
BPD-227	726.9	321.9	1,048.8	2.3
BPD-300	728.9	311.0	1,039.9	2.3
BPD-327	724.9	317.2	1,042.1	2.3
BPD-427	722.9	310.4	1,033.3	2.3
BPD-527	708.9	326.6	1,035.5	2.2
BPD-627	728.9	308.8	1,037.7	2.4
BPD-707	730.9	329.0	1,059.9	2.2
BPD-712	726.9	324.1	1,051.0	2.2
BPD-715	720.9	327.9	1,048.8	2.2
Analytical Detection Limit	0.053	0.109	0.026	0.034

Samples collected May 5, 6, and 7, 1998.
All analyses performed by J. Jonas at the Kelley Mine Analytical Facility.

Table 4-4. Water Properties of Berkeley Pit Lake Water as a Function of Depth (Ref. 9)

Sample (BPD-sampling depth)	Properties				
	TEC	pH	DO, ppm	E_h, mV	Turbidity, NTU
BPD-0.5	14.8	2.7	0.23	444	
BPD-01	14.6	2.7	0.13	444	
BPD-02	13.9	2.7	0.16	443	
BPD-04	12.5	2.6	0.04	443	
BPD-06	12.0	2.6	0.04	441	
BPD-08	10.2	2.6	0.05	431	
BPD-10	7.5	2.6	0.04	418	
BPD-12	6.5	2.6	0.06	414	
BPD-14	6.1	2.6	0.08	411	
BPD-16	6.0	2.6	0.09	411	
BPD-18	5.2	2.6	0.11	406	
BPD-20	4.8	2.6	0.17	404	
BPD-25	4.6	2.6	0.37	404	12.8
BPD-50	4.2	2.5	0.31	400	8.7
BPD-100	4.3	2.5	0.41	399	6.2
BPD-200	4.4	2.5	0.24	399	7.5
BPD-227	5.9	2.4	0.14	401	
BPD-300	4.4	2.5	0.20	399	8.1
BPD-327	5.9	2.4	0.15	401	
BPD-427	6.6	2.4	0.23	401	
BPD-527	6.4	2.4	0.17	401	
BPD-627	6.1	2.5	0.17	403	
BPD-707	5.6	2.5	0.34	402	
BPD-712	6.2	2.5	0.26	402	
BPD-715	6.1	2.5	0.21	402	

Note:
1. Field data collected by MBMG.
2. Samples BPD-627 to 715 were collected May 5; BPD-227 to 627 were collected May 6; BPD-25 to 227 were collected May 7; and BPD 0.5 to 25 were collected May 5, 1998.
3 Data for samples deeper than 100 ft were collected by vertical samplers. Water from the specified depth was pushed (by nitrogen) through the flow cell of the submerged hydrolab. All lines were insulated; however, temperatures are suspect for the +100 ft data.

Table 4-5. Composition of Deep Water and Core One Pore Water (Element Set One)

Sample Slice, cm	Concentration, mg/L (ppm)							
	Al	Ca	Fe	K	Mg	Na	P	Si
				Deep Water, 717 ft				
BPD-1-AVG	293	477	1,097	8.2	491	110	0.8	54
				Core One				
0-5	185	454	2,477	4.4	482	182	0.4	50
5-10	154	442	2,834	4.0	474	105	0.5	49
10-15	129	428	2,707	2.0	458	74	0.5	48
15-20	126	429	2,392	1.4	450	93	0.5	50
20-25	145	431	2,009	1.4	465	90	0.4	53
25-35	187	431	1,609	1.3	458	100	0.2	61
35-45	217	441	1,319	1.6	443	95	0.5	66
55-60	225	439	1,284	2.4	456	99	0.3	65
60-65	228	441	1,247	1.7	461	106	0.4	66
65-69	222	436	1,221	2.9	445	100	0.4	70

Note: Samples were collected April 22, 1998.
All analyses were performed by Dr. W. Chatham and his coworkers at the Kelley Mine Analytical Facility.

Table 4-6. Composition of Deep Water and Core One Pore Water (Element Set Two)

Sample Slice, cm	Concentration, mg/L (ppm)							
	As	Cd	Cu	Mn	Ni	Pb	S	Zn
				Deep Water, 717 ft				
BPD-1-AVG	0.89	2.4	191	235	1.2	0.04	2,825	646
				Core One				
0-5	0.03	2.5	197	232	1.2	0.05	3,432	621
5-10	0.17	2.5	196	235	0.0	0.20	3,454	613
10-15	0.22	2.4	186	226	1.1	0.32	3,358	588
15-20	0.12	2.4	187	220	1.1	0.09	3,091	586
20-25	0.10	2.4	247	217	1.2	0.06	2,966	601
25-35	0.13	2.3	347	211	1.2	0.07	2,794	599
35-45	0.16	2.2	381	210	1.1	0.09	2,631	603
55-60	0.07	2.3	410	208	1.3	0.04	2,680	601
60-65	0.11	2.3	420	207	1.3	0.03	2,729	598
65-69	0.20	2.2	409	203	1.1	0.10	2,637	590

Note: Samples collected April 22, 1998.
All analyses were performed by Dr. W. Chatham and his coworkers at the Kelley Mine Analytical Facility.

Table 4-7. Composition of Deep Water and Cores Two and Three Pore Water (Element Set One)

Sample Slice, cm	Concentration, mg/L (ppm)							
	Al	Ca	Fe	K	Mg	Na	P	Si
				Deep Water, 717 ft				
BPD-1-AVG	293	477	1097	8	491	110	0.8	54
				Core Two				
0.0	177	442	2,636	1.1	485	82	0.6	51
36194.0	195	436	2,734	1.3	533	86	0.6	57
36255.0	158	434	2,881	0.7	473	78	0.3	49
36318.0	135	439	3,141	1.1	459	70	0.3	51
36381.0	140	438	3,244	1.6	544	78	0.3	60
18-20	110	433	3,150	1.3	471	64	0.3	50
45-47	123	445	2,246	1.7	432	76	0.4	53
67-72	207	442	1,377	1.3	435	93	0.2	64
				Core Three				
0.0	140	442	2,618	0.9	455	73	0.2	51
45-50	222	443	1,288	2.3	450	101	0.3	69
75-80	215	435	1,239	2.0	448	89	0.4	68

Note: Samples collected April 22 and 23, 1998.
All analyses were performed by Dr. W. Chatham and his coworkers at the Kelley Mine Analytical Facility.

Table 4-8. Composition of Deep Water and Cores Two and Three Pore Water (Element Set Two)

Sample Slice, cm	Concentration, mg/L								
	As	Cd	Co	Cu	Mn	Ni	Pb	S	Zn
					Deep Water, 717 ft				
BPD-1-AVG	0.89	2.4	1.7	191	235	1.2	0.04	2,825	646
					Core Two				
0-2	0.13	2.5	1.9	198	229	1.3	0.12	3,517	611
2-4	0.08	2.7	1.9	214	229	1.3	0.04	3,887	614
4-6	0.02	2.5	1.7	193	231	1.1	0.06	3,546	608
6-8	0.04	2.4	1.7	196	232	1.4	0.06	3,555	606
8-10	0.10	2.9	2.0	227	232	1.5	0.14	4,242	608
18-20	0.04	2.5	1.8	199	227	1.3	0.12	3,639	597
45-47	0.36	2.3	1.6	195	216	1.1	0.20	2,953	581
67-72	0.12	2.2	1.6	367	206	1.2	0.04	2,645	593
					Core Three				
0-5	0.05	2.4	1.7	202	221	1.2	0.04	3,336	590
45-50	0.21	2.2	1.5	390	206	1.1	0.08	2,713	592
75-80	0.19	2.3	1.8	428	201	1.2	0.08	2,693	585

Note: Samples collected April 22 and 23, 1998.
All analyses were performed by Dr. W. Chatham and his coworkers at the Kelley Mine Analytical Facility.

Table 4-9. Iron Speciation in Pore Waters for Cores One, Two, and Three (Ref. 8)

Sample	Slice, cm	Concentration, mg/L			
		Fe^{+2}	Total Fe	Fe^{+3}	Fe^{+2}/Fe^{+3}
		Core One			
BPD-C1-CS1	0-5	2,434	2,608	174	14
BPD-C1-CS2	5-10	2,742	2,932	191	14
BPD-C1-CS3	10-15	2,766	2,981	215	13
BPD-C1-CS4	15-20	2,386	2,457	72	33
BPD-C1-CS5	20-25	1,878	2,022	144	13
BPD-C1-CS6	25-35	1,406	1,565	159	9
BPD-C1-CS7	35-45	1,158	1,298	141	8
BPD-C1-CS8	55-60	1,078	1,210	132	8
BPD-C1-CS9	60-65	1,082	1,219	137	8
BPD-C1-CS10	65-69	1,042	1,179	137	8
		Core Two			
BPD-C2-CS1	0-2	2,658	2,852	195	14
BPD-C2-CS2	2-4	2,674	2,892	219	12
BPD-C2-CS3	4-6	2,890	3,110	220	13
BPD-C2-CS4	6-8	3,094	3,332	238	13
BPD-C2-CS5	8-10	3,222	3,447	226	14
BPD-C2-CS7	18-20	3,126	3,349	224	14
BPD-C2-CS11	45-47	2,154	2,333	179	12
BPD-C2-CS14	67-72	1,186	1,347	162	7
		Core Three			
BPD-C3-CS1	0-5	2,534	2,710	177	14
BPD-C3-CS6	45-50	1,118	1,267	150	7
BPD-C3-CS10	75-80	1,014	1,187	174	6

Note: All analyses were performed by J. Jonas at the Kelley Mine Analytical Facility.

Table 4-10. Properties of Pore Waters in Cores One, Two, and Three

Sample ID	Slice, cm	$E_{Ag/AgCl}$, mv	pH	DO, ppm
		Deep Water, 717 ft		
BPD-1	-	357	3.1	0.2
		Core One		
BPD-C1-CS1	0-5	357	3.1	0.2
BPD-C1-CS2	5-10	327	3.1	0.2
BPD-C1-CS3	10-15	305	3.2	0.4
BPD-C1-CS4	15-20	273	3.3	0.3
BPD-C1-CS5	20-25	265	3.4	0.2
BPD-C1-CS6	25-35	287	3.3	0.2
BPD-C1-CS7	35-45	284	3.3	0.3
BPD-C1-CS8	55-60	282	3.3	0.3
BPD-C1-CS9	60-65	282	3.3	0.3
BPD-C1-CS10	65-69	283	3.3	NA
		Core Two		
BPD-C2-CS1	0-2	316	3.1	0.3
BPD-C2-CS2	2-4	332	3.1	0.4
BPD-C2-CS3	4-6	303	3.2	0.4
BPD-C2-CS4	6-8	290	3.2	0.3
BPD-C2-CS5	8-10	284	3.2	0.4
BPD-C2-CS7	18-20	280	3.2	0.4
BPD-C2-CS11	45-47	270	3.3	0.3
BPD-C2-CS14	67-72	286	3.2	0.4
		Core Three		
BPD-C3-CS1	0-5	313	3.2	0.4
BPD-C3-CS6	45-50	279	3.3	0.4
BPD-C3-CS10	75-80	275	3.3	0.4

Note: All analyses were performed by Dr. W. Chatham and his coworkers at the Kelley Mine Analytical Facility.

Table 4-11. Chemical Composition of Deep Water Sediment Surface Solids

Element	Composition, %		
	600 ft	700 ft	717 ft (Core One, surface solid)
Fe	13.2	22.2	15.5
Si	16.8	11.0	13.3
Al	7.0	6.2	6.1
S	3.2	4.8	4.3
K	1.9	1.6	1.6
Mg	0.8	0.7	0.8
Ca	0.7	0.5	0.6
Cu	0.4	0.3	0.3
Ti	0.3	0.2	0.3
Zn	0.2	0.2	0.2
As	0.1	0.2	0.1
Na	U	0.1	0.0
Pb	0.1	0.1	0.1
Mn	0.1	0.1	0.1
Ba	0.0	0.0	0.0
P	0.0	0.0	0.0
V	0.0	0.0	0.0
Sr	0.0	0.0	0.0
Mo	0.0	0.0	0.0
Cr	0.0	0.0	0.0
Sb	0.0	0.0	0.0
Zr	0.0	0.0	0.0

Note: All analyses were performed by Dr. W. Chatham and his coworkers at the Kelley Mine Analytical Facility.
Elemental analyses performed using Method 3052A.

Table 4-12. Elemental Composition of Core One Solids as a Function of Core Depth

Element	Composition of Core One Slices, %									
	0-5 cm	5-10 cm	10-15 cm	15-20 cm	20-25 cm	25-35 cm	35-45 cm	55-60 cm	60-65 cm	65-69 cm
Al	6.06	6.25	6.34	5.32	5.89	8.07	7.31	5.22	5.27	6.60
As	0.11	0.10	0.12	0.14	0.07	0.15	0.07	0.06	0.07	0.07
Ba	0.03	0.03	0.03	0.02	0.03	0.03	0.02	0.01	0.01	0.02
Ca	0.60	0.66	0.70	0.53	0.72	0.67	0.53	0.45	0.43	0.50
Cd	<DL	<DL	<DL	<DL	<DL	<DL	<DL	<DL	<DL	<DL
Cu	0.25	0.24	0.29	0.29	0.31	0.43	0.51	0.52	0.62	0.69
Fe	15.46	11.72	12.42	10.02	7.47	10.03	7.23	6.81	6.47	6.80
K	1.57	1.57	1.60	1.57	1.75	1.76	1.38	1.05	1.06	1.21
Mg	0.79	0.77	0.86	0.47	0.55	0.79	0.69	0.37	0.54	0.73
Mn	0.08	0.07	0.08	0.07	0.06	0.06	0.07	0.07	0.07	0.08
Na	<DL	<DL	<DL	0.14	0.20	0.64	0.01	<DL	2.18	<DL
P	0.05	0.03	0.05	0.04	U	0.05	0.03	<DL	0.02	0.01
Pb	0.07	0.07	0.13	0.11	0.08	0.07	0.05	0.05	0.05	0.06
S	3.52	2.82	3.31	2.96	2.95	2.17	1.18	0.99	1.15	1.32
Si	13.28	14.90	16.01	17.39	20.26	20.26	20.33	18.96	17.50	19.01
Ti	0.27	0.29	0.33	0.35	0.34	0.34	0.33	0.33	0.31	0.32
V	0.02	0.01	0.02	0.01	0.01	0.01	U	0.01	0.01	0.01
Zn	0.16	0.14	0.23	0.15	0.13	0.14	0.17	0.15	0.18	0.21

Note: All analyses were performed by Dr. W. Chatham and his coworkers at the Kelley Mine Analytical Facility.
Elemental analyses performed using Method 3052A.
DL=detection limit.

Table 4-13. Elemental Composition of Cores Two and Three Solids as a Function of Core Depth

Element	Composition of Cores Two and Three Slices, %										
	Core Two								Core Three		
	0-2 cm	2-4 cm	4-6 cm	6-8 cm	8-10 cm	18-20 cm	45-47 cm	67-72 cm	0-5 cm	45-50 cm	75-80 cm
Al	12.43	5.43	6.56	6.68	7.47	6.67	7.18	7.31	7.01	4.54	7.30
As	0.25	0.11	0.13	0.09	0.06	0.08	0.16	0.07	0.09	0.07	0.04
Ba	0.07	0.03	0.04	0.04	0.04	0.03	0.02	0.02	0.03	0.01	0.01
Ca	1.30	0.58	0.66	0.61	0.76	0.52	0.44	0.49	0.65	0.30	0.55
Cd	<DL	<DL	<DL	<DL	<DL	<DL	<DL	<DL	<DL	<DL	<DL
Cu	0.52	0.20	0.28	0.33	0.28	0.23	0.31	0.54	0.31	0.52	0.36
Fe	29.18	13.61	14.83	13.16	9.00	12.84	11.18	6.71	12.64	5.63	6.86
K	3.22	1.57	1.68	1.47	1.93	1.62	1.80	1.40	1.59	0.83	1.34
Mg	1.64	0.59	0.84	0.90	0.98	0.81	0.70	0.79	0.87	0.46	0.47
Mn	0.13	0.06	0.06	0.06	0.06	0.08	0.07	0.07	0.07	0.06	0.08
Na	<DL	<DL	<DL	<DL	<DL	<DL	0.46	<DL	<DL	<DL	<DL
P	0.08	<DL	0.04	0.02	0.03	0.02	0.06	<DL	0.03	0.04	<DL
Pb	0.15	0.05	0.07	0.07	0.04	0.08	0.13	0.05	0.10	0.06	0.03
S	6.77	2.89	3.80	2.80	1.89	2.42	2.95	1.23	2.84	0.99	0.62
Si	31.22	13.22	18.94	15.99	21.78	17.51	15.77	18.16	16.62	17.69	20.59
Ti	0.51	0.26	0.27	0.26	0.31	0.31	0.30	0.32	0.31	0.25	0.32
V	0.04	0.01	0.02	0.01	0.01	0.01	0.01	0.01	0.02	<DL	0.01
Zn	0.30	0.10	0.12	0.13	0.11	0.14	0.15	0.16	0.18	0.15	0.10
C[1]	<DL										<DL
C[2]	0.30										0.40

Note: All analyses were performed by Dr. W. Chatham and his coworkers at the Kelley Mine Analytical Facility.
Elemental analyses performed using Method 3052A.
DL=detection limit.
1 Inorganic carbon; DL=0.1%
2 Organic carbon; DL=0.1% (determined by combustion in oxygen with subsequent analysis of carbon dioxide by nondispersive infrared).

Table 4-14. Sediment Solids Content for Cores One, Two, and Three

Sample ID	Slice, cm	Solids Content, %	Specific Gravity, g/cc
	Core One		
BPD-1-CS-1	0-5	2.8	2.8
BPD-1-CS-2	5-10	17.1	
BPD-1-CS-3	10-15	27.8	
BPD-1-CS-4	15-20	41.4	
BPD-1-CS-5	20-25	47.0	
BPD-1-CS-6	25-35	43.7	
BPD-1-CS-7	35-45	44.8	
BPD-1-CS-8	55-60	44.5	
BPD-1-CS-9	60-65	44.3	
BPD-1-CS-10	65-69	45.8	
	Core Two		
BPD-2-CS-1	0-2	22.2	
BPD-2-CS-2	2-4	32.9	
BPD-2-CS-3	4-6	34.2	
BPD-2-CS-4	6-8	36.1	
BPD-2-CS-5	8-10	46.0	
BPD-2-CS-7	18-20	37.0	
BPD-2-CS-11	45-47	40.9	
BPD-2-CS-14	67-72	45.8	
	Core Three		
BPD-3-CS-1	0-5	28.6	
BPD-3-CS-6	45-50	43.6	
BPD-3-CS-10	75-80	48.2	2.7

Note: Average of three separate determinations.
All determinations performed by R. J. Ziolkowski in the Montana Tech Metallurgical Engineering Department.

Table 4-15. Ratio of Phase Area to Quartz Area for Sediment Solids

Mineral	Sediment Surface[1]		Core[1]	
	600 ft 11/18/97	700 ft 11/20/97	717 ft 4/22,23/98	
			Core Two Top	Core Three Bottom
Quartz	1	1	1	1
Jarosite	0.3	0.8	0.3	0.2
Gypsum	-	0.3	0.2	0.1
Biotite	-	0.3	0.4	0.2
Muscovite			0.2	0.4

Note: Area under major peak for each phase/area under the major quartz peak

Table 4-16. Mineralogy of Sediment/Deep Water Interface Samples (600 ft, 700 ft, and Robins 700 ft)

Sample	Precipitated Components	Detrital Components										
	Jar	Gyp	Quar	Bio	Plag	Ser	Mus	Py	Hem	Zir	Apat	Horn	Ep
600 ft	M	m	M	m	tr	tr	tr	tr					
700 ft	M	tr	M	m	-	tr	tr	tr			tr		
700 ft, Robins	M	m	M	m	tr	m	tr	tr	tr	tr	tr(?)	tr	tr

Note: Jar=jarosite, Gyp=gypsum, Quar=quartz, Bio=biotite, Plag=plagioclase, Ser=sericite, Mus=muscovite, Py=pyrite, Hem=hematite, Zir=zircon, Apat=apatite, Horn=hornblende, Ep=epidote.
M=major, m=minor, tr=trace.

Note: Jarosite was identified by XRD analysis and was substantiated by EDX. Gypsum was confirmed by EDX. Smectite and kaolinite were tentatively identified by XRD analysis of the fine fraction of sample 700 ft. Further analysis of clay mineralogy would have required an additional amount of sample.

Identifications were performed by R.B. Berg (MBMG).

Table 4-17. Observations Made by Petrographic Examination for Sediment/Deep Water Interface Samples (600 ft, 700 ft, Robins 700 ft)

Mineral	Observation
Detrital Component	
Quartz	Quartz was the most abundant detrital component being a major phase in all samples. Quartz grains are angular to subrounded, generally coated with jarosite, and most grains were between 20 to 80 µm. Some of the quartz grains derived from veins contained an abundance of small fluid inclusions.
Biotite	Biotite flakes were tan to brown in basal orientation had an irregular to slightly rounded outline, and were present in all samples. The flakes ranged from 40 to 80 µm in maximum dimension.
Plagioclase	Angular grains of unaltered plagioclase were found in trace concentrations in samples 600 ft and 700 ft (Robins). Identification was based on morphology and EDX results showing sodium, calcium, aluminum, silicon, and oxygen.
Sericite	Irregular composite flakes of sericite (a fine-grained muscovite that occurs next to quartz veins in the orebody) were present in low concentrations and ranged up to 75 µm in size.
Muscovite	Individual muscovite flakes were present in trace concentrations. The maximum dimension was 80 µm.
Pyrite	Irregular pyrite grains, some with a conchoidal fracture, were recognized by their shiny, brassy luster when examined in reflected light. Pyrite grains were present in trace concentrations. Identified grains ranged from 40 to 95 µm.
Other Minerals	Other minerals found only in trace concentrations included hematite, zircon, apatite, epidote, and hornblende.
Precipitated Component	
Jarosite	Aggregates of small (1 to 2 µm) globular grains occurred in discrete masses up to 0.8 millimeters (mm) across and also were adhering to both the detrital component and gypsum crystals. Petrographic examination of these globular grains with crossed nicols showed a radial pattern of individual jarosite grains within the globules. In immersion mounts, jarosite appeared to be the most abundant constituent in all the samples.
Gypsum	Gypsum crystals showed the typical prismatic outline of the variety selenite and ranged from 20 to 140 µm in length. No evidence of abrasion or etching of this mineral was observed, which suggests that the gypsum was precipitated. Jarosite was found adhering to the gypsum surface, and it is inferred that the gypsum formed first or contemporaneous with jarosite forming as the gypsum crystals settled to the bottom of the Pit.

Mineral	Observation

Note: Observations were performed by R.B. Berg (MBMG).

Table 4-18. Mineralogy of Core Two and Core Three Sediments as a Function of Core Depth (collected April 23, 1998)

Sample	Precipitated Components		Detrital Components	
	Jarosite	Gypsum	Quartz	Biotite
	Core Two			
BPD-C2-CS1 (Top)	M	m	M	m
BPD-C2-CS4	M	m	M	m
BPD-C2-CS6	M	m	M	m
BPD-C2-CS8	M	m	M	m
BPD-C2-CS10	M	m	M	m
BPD-C2-CS14 (Bottom)	M	m	M	m
	Core Three			
BPD-C3-CS1 (Top)	M	m	M	m
BPD-C3-CS2	M	m	M	m
BPD-C3-CS5	M	m	M	m
BPD-C3-CS7	M	m	M	m
BPD-C3-CS9	M	m	M	m
BPD-C3-CS10 (Bottom)	M	m	M	m

Note: M=major; m=minor; tr=trace
Note: Jarosite was identified by XRD analysis and was substantiated by EDX. Gypsum was confirmed by EDX.
Identification work was performed by R. J. Ziolkowski (Montana Tech Metallurgical Engineering Department)
Further evaluative work is presently being conducted to identify minor and trace components (Ref. 6).

Table 4-19. Observations Made by Petrographic Examination for Core Two and Core Three Sediments (Samples Collected April 23, 1998)

Sample	Size, μm[1]		
	Gypsum	Biotite	Quartz
	Core Two		
BPD-C2-CS1 (Top)	78x70	78x102	170x370
BPD-C2-CS4	80x30	85x14	53x85
BPD-C2-CS6	40x20	100x85	60x50
BPD-C2-CS8	45x15	55x55	45x65
BPD-C2-CS10	53x14	83x75	50x50
BPD-C2-CS14 (Bottom)	30x8	180x80	38x22
	Core Three		
BPD-C3-CS1 (Top)	48x10	110x50	46x37
BPD-C3-CS2	76x9	125x82	37x21
BPD-C3-CS5	49x10	140x106	636x40
BPD-C3-CS7	43x12	167x116	32x25
BPD-C3-CS9	108x32	380x96	45x108
BPD-C3-CS10 (Bottom)	152x51	180x193	140x 88

Table 4-19. Observations Made by Petrographic Examination for Core Two and Core Three Sediments (Samples Collected April 23, 1998)

Sample	Size, µm[1]		
	Gypsum	Biotite	Quartz

1 length by width, all reported values are an average of three-dimension determinations.
All size determinations were performed by R. J. Ziolkowski.

Table 4-20. SEM-EDX Study on 600-ft Sediment-Surface Solids and Selected Core Samples

Description	Composition, % (semiquantitative)								
	Al	Ca	Fe	Mg	Na	K	O[1]	S	Si
C2-CS1 (Surface of Sediment)									
Bulk	6.2		25.6	0.8		2.5	40.8	11.2	12.8
Sample Particle: Biotite	9.1		8.2	8.5		7.0	45.6		20.1
Sample Particle: Pyrite			41.5					58.5	
Particle: Gypsum		19.4	2.8				58.6	15.9	2.6
(+325 mesh) Sample Particle: Biotite	8.2		10.7	7.3		7.1	44.8		20.3
(+325 mesh) Sample Particle: Plagioclase	13.8	6.6			5.9		47.2		26.4
(-325 mesh) Sample Bulk	3.8		13.4	0.5	0.7	2.4	63.2	2.7	9.7
(-325 mesh) Sample Particle: Quartz	0.5		1.4				56.2		41.9
(-325 mesh) Sample Particle: Iron Aluminum Silicate	2.9	0.3	5.9	0.5		2.0	62.0	0.9	14.4
C2-CS11 (Bottom of Core Two)									
Bulk	11.8		14.2	0.8		4.9	43.2	4.6	20.6
Bulk	10.1		11.9	1.3		3.7	45.9	3.3	23.8
Bulk	13.2		9.8	0.9		3.0	46.6	3.3	23.3
C3-CS10 (Bottom of Core Three)									
Bulk	12.6		9.6	1.6		3.4	46.3	1.2	25.4
Sample Particle: Biotite	8.7		12.3	7.8		8.5	40.9	0.3	19.6
(+325 mesh) Sample Particle: Quartz		1.1					53.3		45.6
(+325 mesh) Sample Particle: Apatite		42.8					37.4	P=19.8	
(+325 mesh) Sample Particle: Albite	13.6				6.3		59.7		28.2
(+325 mesh) Sample Particle: Potassium Aluminum Silicate	18.0		1.4	0.7	0.2	9.0	47.6		23.1
(+325 mesh) Sample Particle: Biotite	4.0		9.3			2.3	57.0	1.9	15.3
600 ft (Surface Sediment Solid)									
Sample Particle: Gypsum	1.4	19.0		1.9			57.0	17.9	2.2
Sample Particle: Plagioclase Feldspar	11.3	3.4			7.2		49.1		29.0
Sample Particle: Biotite	10.4		13.5	8.5		1.9	59.9		22.2
Jarosite on Biotite	5.3		32.8	3.8		2.6	39.1	6.0	10.3
Jarosite on Biotite	4.9	1.0	44.8			2.7	44.8	4.0	8.0

Note: C2-CS1= Core Two, slice one (top of core).
C2-CS11=Core Two, slice eleven (bottom of core).
C3-CS10=Core Three, slice ten (bottom of core, deepest sediment sample collected).
600 ft=Sample collected from the surface of the sediment from a water depth of 600 ft.

Table 4-21. Comparison of Shallow, Deep, and Pore Water Chemistry

Sample	Concentration, mg/L (ppm)														
	Al	As	Ca	Cd	Cu	Fe	K	Mg	Mn	Na	P	Pb	S	Si	Zn
BPS-1	283	0.8	437	2.5	184	1027	7	466	218	104	0.8	0.1	3100	56	602
BPD-1	293	0.9	477	2.4	191	1097	8	491	235	111	0.8	0.0	2825	54	646
BPD-C1-CS1	185	0.0	454	2.5	197	2477	4	482	232	182	0.4	0.1	3432	50	621
BPD-C3-CS10	215	0.2	435	2.3	428	1239	2	448	201	89	0.4	0.1	2693	68	585

BPS=Berkeley Pit shallow, 160 ft
BPD=Berkeley Pit deep, 717 ft
BPD-C1-CS1=pore water from the sediment/water interface.
BPD-C3-CS10=pore water from the deepest sediment sample collected.
All analyses performed by Dr. W. Chatham and his coworkers at the Kelley Mine Analytical Facility.

Table 4-22. Resident Conditions in Pore Water for Core One, Top Slice

Element	Concentration, mg/L	
	mg/L	M/L
Al	185	6.86E-03
Ca	454	1.19E-02
Fe (II) (ferrous)	2477	4.35E-02
K	4.4	1.12E-04
Mg	482	1.98E-02
Si	50	1.78E-03
	mg/L	**M/L**
Cu	197	3.10E-03
S	2825	1.07E-01
Zn	646	9.50E-3

Solution pH=3.1
Ionic Strength=0.218 moles/L
E_H=0.6 V (calculated)

Table 4-23. Activities for Speciated Products used in the Free Energy Calculation

Specie	Activity, moles/L
HCO_3^{-1}	1.74E-04
Fe^{+2}	7.08E-05
SO_4^{-2}	1.50E-02
K^{+1}	7.44E-05

5. Quality Assurance/Quality Control

This project was conducted to characterize sediments collected from the deepest location in the Berkeley Pit. Pore water and sediment solids were characterized. The programmatic and regulatory setting in which the project QA was conducted was Category III.

The QAPP used in this study complied with the requirements of a Category III project plan. Category III projects are those producing results to be used to evaluate and select basic options or to perform feasibility studies or preliminary assessments of unexplored areas.

5.1 QAPP Objective

The QA/QC objectives outlined for the project were specified to generate acceptable Category III data. The QAPP is presented in detail in Reference 6. Briefly, the QAPP was designed to demonstrate the following:

- intended measurements are appropriate for achieving project objectives;
- quality control procedures are sufficient for obtaining data of known and adequate quality; and
- such data are defensible if challenged technically.

5.2 Analytical Procedures and Calibration

5.2.1 EPA-Approved Methods

Solutions: Waters and Digested Solutions
Solutions were analyzed at Montana Tech (Kelley Mine Analytical Facility) using a Perkin Elmer Optima ICP according to EPA SW 836, Method 6010A.[1] Solution samples were prepared for ICP analysis according to the procedures outlined in SW 836, Method 3005A. Digested samples were prepared according to Method 3050A.

Solids
X-ray diffraction analyses were performed using a Phillips 3100 x-ray generator.

5.2.2 Equipment Calibration

ICP Calibration
The ICP instrument was calibrated according to the procedures outlined in EPA SW 846, Method 6010A and the equipment manufacturer's recommendations. The acid matrix for the ICP calibration standards was matched to the matrix used to prepare the samples. The internal QC checks for ICP included:

- instrument calibration (IC);
- initial and continuing calibration verifications (ICV and CCV);
- initial and continuing calibration blanks (ICB and CCB);
- preparation blank (PB);
- matrix spike;
- analytical duplicate samples;
- serial dilution analysis;
- laboratory control sample (LCS);
- interelement correction (ICSA and ICSAB); and
- instrument detection limit (IDL) determination (determined quarterly).

pH and E_H meters
The pH and E_H meters calibration followed the manufacturer's recommended procedures (ORION). Two buffer solutions were used for calibration. Zobell's solution was used to verify that the E_H probe was performing correctly, i.e., the Zobell's solution produces a potential reading (using a silver/silver chloride/platinum probe) of 436 mV at 20 EC. If the reading of the standard solution fell outside of a range of ±35 mV then the probe was cleaned, and the fill solution was replaced. The calibration checks for the pH and

E_H meters and probes included an ICV and a CCV every hour of instrument operation.

X-Ray Diffraction
The XRD system was calibrated using a National Institute of Standards and Testing reference material, i.e., SRM 1976, alumina. The calibration verification procedure was performed on a quarterly basis.

5.3 Data Validation

Quality assurance objectives for sampling events conducted in November 1997 and April 1998 are summarized in Table 5-1.

Table 5-1. Quality Assurance Objectives for Analytical ICP Data

Parameter	Accuracy[1]	Completeness[2]	Precision[3]
Dissolved Elements	±25%	80%	#20% RPD

1 Accuracy=(sample concentration/concentration in laboratory control sample, LCS)*100
2 Completeness=(samples judged valid/No. samples)*100
3 Precision (RPD)=(different in dupl. concentrations/average of dupl. concentrations)*100

5.3.1 November Sampling Event
The attainment of QA objectives for the November 18 and 20 sampling events are summarized in Table 5-2. Solution concentration data is summarized in Appendix B, Tables B.1-1 through B.1-4. The experimental procedures used are presented in the QAPP (Ref. 1).

The validation summary report for completeness, accuracy, and precision results of the November sampling events are presented in Table 5-2. All three QA objectives (Table 5-1) were satisfied for all elements. The accuracy of all elemental analyses fell within the required range of ±25% (except for one potassium analysis). Potassium was accepted because it met the precision criteria.

The precision (#20% RPD) for all elemental analyses met the desired quality objective.

5.3.2 April Sampling Events

The attainment of QA objectives for the April 22 and 23, 1998, sampling events are summarized in Table 5-3. Solution concentration data is summarized in Appendix B, Tables B.2-1 through B.2-7.

The validation summary report for completeness, accuracy, and precision results of the April sampling events are presented in Table 5-3. All three QA objectives (Table 5-1) were satisfied for all elements. The accuracy of all elemental analyses fell within the required range of ±25%. The precision (#20% RPD) for all elemental analyses met the desired quality objective except for one analyses for lead in the pore water. Lead was accepted as valid because it showed acceptable accuracy.

Solution pH (a noncritical measurement) was determined in an argon atmosphere glovebox. The pH was monitored using an Orion 940 pH meter. The accuracy of the measurements was ensured by careful calibration and recalibration of the pH probe every 10 samples.

Temperature in the laboratory glove box was not controlled. The temperature range was 20 to 28 EC. All samples were sealed under argon and stored at 4 EC.